

Propagation of sound and second sound using heat pulses

V. Narayanamurti, R. C. Dynes, and K. Andres

Bell Laboratories, Murray Hill, New Jersey 07974

(Received 29 July 1974)

We present a detailed account of the transition from second sound to ballistic phonon flow in liquid He II as a function of temperature (0.1–1 K), pressure (up to the solidification point), and propagation length (~ 0.23 – 7.0 cm). Below 10 bar and 0.5 K, the phonon-phonon scattering time τ_{pp} has the form $\tau_{pp} \sim (7 \pm 3) \times 10^{-11}(T/\Theta)^{-3}$ sec, where Θ is the low-temperature Debye temperature. Above 10 bar, $v\tau_{pp} > 2$ cm for $T \lesssim 0.7$ K, where v is the sound velocity. The strong pressure dependence of τ_{pp} is qualitatively consistent with the theoretical model of Jäckle and Kehr. The phonon-roton scattering time τ_{pr} is found to be nearly pressure independent and has a value $\sim 10^{-6}$ sec at ~ 0.75 K in agreement with the calculations of Khalatnikov and Chernikova. Evidence for separate roton second sound (at high pressures) and phonon second sound at SVP is presented. An elementary excitation picture of second sound in the entire gas of excitations in He II is presented and the close analogy with phonon second sound in solids (bismuth) and in a gas of particles (He^4) is experimentally illustrated. Estimates for the number of collisions required for the formation of the collective mode from the single-particle-like excitations are given.

I. INTRODUCTION

The possibility that temperature variations can propagate as collective waves (second sound) was first proposed by Tisza¹ and by Landau^{2,3} for the case of superfluid He⁴. Using two-fluid hydrodynamics, Landau showed that the velocity of second sound, v_{II} , in He II depended strongly on the temperature T via the expression

$$v_{II}^2 = (TS^2/C)(\rho_s/\rho_n), \quad (1)$$

where S is the entropy, C the specific heat, and ρ_s and ρ_n the superfluid and normal fluid densities. He showed that v_{II} depended markedly on the temperature through the strong T dependence of the different thermodynamic quantities occurring in (1). The strong temperature dependence of C , S , ρ_s , and ρ_n (and hence v_{II}) was postulated by Landau to be due to the existence of a high-energy branch (roton branch) in the He I excitation spectrum. At high temperatures (above about 0.7 K) v_{II} is small (~ 20 m/sec) because of the thermal population of low-group-velocity rotonlike excitations. At low temperatures, when the only excitations are phonons, Landau showed that v_{II} is independent of temperature and reaches the limiting value $v_{II} = v_1/\sqrt{3}$ [where v_1 is the velocity of first sound (~ 240 m/sec) at saturated vapor pressure (SVP)]. In 1951, Ward and Wilks⁴ extended some of Landau's ideas and gave a *microscopic* description of second sound in He II at low temperatures in terms of the elementary excitations (phonons). They assumed strong interactions amongst the excitations and that these interactions conserve energy and momentum. Using these assumptions they solved the phonon Boltzmann equation and showed that variations in the number density of phonons could occur in a

periodic manner, traveling with a velocity $v_{II} = v_1/\sqrt{3}$. In their paper, Ward and Wilks also extended the idea of second sound in the phonon gas in He II to the case of dielectric solids, where the only excitations are phonons but where momentum-destroying resistive processes make the observation of an undamped temperature wave more difficult. This subject lay essentially dormant till the 1960's when the work of Krumhansl, Prohofsky, and Guyer^{5,6} put the concept of second sound in solids on a firm theoretical foundation and showed clearly the existence of a temperature (frequency) window for the observation of this phenomenon depending on the relative values of momentum conserving and momentum destroying collision processes. They also briefly discussed⁵ the close analogy between sound propagation in a classical gas (periodic fluctuations in the number density of particles) and second sound in the phonon gas (periodic fluctuations in the phonon density).

It is important to point out here that the concept of second sound as a well-defined excitation assumes strong scattering among the excitations relative to the frequency of study (propagation time in the case of a pulsed experiment), i.e., $\omega\tau \ll 1$. In the absence of scattering ($\omega\tau \gg 1$), ballistic flow of excitations (particles in the case of a gas) is expected. A study of the transition from the collective mode to the ballistic mode can yield valuable information about the lifetimes τ of the excitations under study.

In this paper we wish to present a detailed account of (i) our studies of the transition⁷ from second-sound propagation to ballistic flow as a function of temperature and pressure (up to the solidification point) in liquid helium II; and (ii) we wish to illustrate *experimentally* the strong interrela-

tionship between second sound in solids⁸ (bismuth), liquids (He II), and gases⁹ (He³ and He⁴). We use the fast-heat-pulse technique¹⁰ for the study of the above phenomena and present experimental criteria for the observation of the collective mode in physical systems of interest. In addition, we give a description of second sound in liquid helium II in terms of its elementary excitations, which is valid in a region where both phonons and rotons are thermally populated. We show that we can get numerical agreement with experimentally observed second-sound velocities using this physically appealing elementary excitation picture.

As is well known, heat-pulse techniques have been used extensively in the past to study second sound in liquid helium, particularly at SVP. The velocity of such pulses above about 0.6 K has been determined accurately.¹¹ At low temperatures, however, mean-free-path effects^{12,13} are known to become very important, and in fact most of the previous measurements were limited either by the use of carbon bolometers with slow response times or by the use of long narrow tubes where boundary collisions were important. Under these conditions most of the heat pulses at low temperatures had a shape characteristic of diffusion. Part of the problem, namely, the influence of the chamber walls, was eliminated in the very careful recent work of Guernsey and Luszczynski¹⁴ who, however, had to still employ rather wide pulse widths because of the continued use of carbon bolometers. The development of fast and highly sensitive superconducting bolometers¹⁰ has enabled us to work with much narrower pulses and shorter propagation distances, so that the energy dissipated per pulse in our work is substantially smaller than was possible previously. The importance of the energy dissipated (amplitude and pulse width) will become clear from the results of this work. Finally, excepting the very early work of Mayer and Herlin,¹⁵ we know of no previous work under pressure in the ballistic and transition regions. As we shall see, the application of pressure has an enormous influence on the scattering rates of excitations and allows us to vary the phonon and roton contributions to the heat flow in a rather controlled way.

The paper is divided into four major parts. Section II gives the theoretical background and the elementary excitation picture of second sound in the three states of matter. Our primary attempt, here, is to give a unified view.

In Sec. III we describe the experimental techniques. Salient features of our experiments are discussed here.

Finally, Sec. IV summarizes our experimental results. The data shown are primarily for liquid helium. We, however, present some data for the solid (bismuth) and gaseous helium to il-

lustrate the experimental connection for the three states of matter. In this section, we also give a brief discussion of our liquid-helium results in the light of current theories of the lifetimes of the elementary excitations and present evidence for the existence of a temperature "window" for observing separate phonon and roton contributions to the heat flow at elevated pressures.

II. THEORETICAL BACKGROUND

In this section we briefly review the salient features of heat-pulse propagation pertinent to our experiments. We present a general discussion of second sound in terms of the elementary excitations for the three states of matter and give, in particular, numerical calculations of the temperature dependence of the second-sound velocity in liquid helium II. We also discuss the effects of finite lifetimes of excitations on the propagation of heat pulses and finally discuss what is known about the lifetimes of the phonon and roton excitations in helium II.

A. Nature of heat-pulse propagation

1. General considerations

Recently, there has been considerable activity¹⁰ in the study of the propagation, particularly in solids of short-duration heat pulses. The usual experimental setup in these experiments consists of three elements: the heater, the sample, and the bolometer detector. As pointed out earlier, the fast-heat-pulse technique uses thin ($\sim 1000\text{-\AA}$ -thick) metal films which have extremely short thermal relaxation times¹⁶ ($\sim 10^{-8}$ sec or less) as generators and detectors. Furthermore, the use of superconducting films as bolometers provides one with an extremely sensitive detector of thermal energy in the temperature range below the T_c of the superconductor. The heater is usually a metallic alloy (constantan, AlMn, disordered Au, for example) so that its temperature coefficient is negligible. The experiment is started at time $t=0$ by passing a short ($\sim 10^{-7}$ sec) current pulse of amplitude I_h through the heater film of resistance R (usually $\approx 50 \Omega$). The heat pulse is received by the detector film after a time of flight t determined by the nature of heat propagation in the sample under study which in turn depends profoundly on the temperature.

At the lowest temperatures, the heat pulse generally travels ballistically and arrives at the detector at times corresponding to rectilinear propagation of the elementary excitations of the medium under study (particles in the case of a gas; phonons and rotons in the case of He II; and longitudinal and transverse phonons in the case of a solid). The shape of the ballistic pulses is governed by the velocity spectrum of the excitations

(group velocity since we are concerned with energy flow). This spectrum in turn depends on the heat-pulse temperature T_h . This quantity is ill-defined in the ballistic region in most of the sample but serves to parametrize the distribution of emitted excitations in a small volume of the order of $A\bar{v}\Delta t$ adjacent to the heater. Here A is the area of the heater, \bar{v} an average velocity of emitted excitations, and Δt the pulse duration. The precise value of T_h may be affected by a variety of substrate and sample conditions, but in general the value of T_h in a given experiment may be varied by a large amount by varying I_h and the dependence of T_h on I_h will be governed by a Stefan-Boltzmann-type radiation law in most instances. Finally, even in the ballistic region, if the detector sensitivity is high, one can probe essentially the ambient excitations of the sample by working with very small heater-pulse currents I_h so that $T_h \approx T_s$, where T_s is the sample temperature.

The propagation of ballistic pulses will as mentioned earlier, only occur as long as the mean free path of the excitations is long compared to the propagation distance L . In the presence of scattering mechanisms, the ballistic flow will be profoundly affected. Neglecting, for the moment, resistive (momentum nonconserving) processes, the effect of collisions among the excitations can be briefly described as follows. In the limit of frequent collisions among the excitations (the mean relaxation time $\bar{\tau}_N$ for normal scattering satisfies the condition $\bar{\omega}\bar{\tau}_N \ll 1$, where $\bar{\omega}$ is some mean frequency characterizing the pulse) a true temperature can be defined within the pulse and heat pulses will travel as undamped second sound.

Several attempts have been made recently to connect theoretically the kinetic (ballistic) to the hydrodynamic (second-sound) region of heat-pulse propagation. The simplest approach, and which has

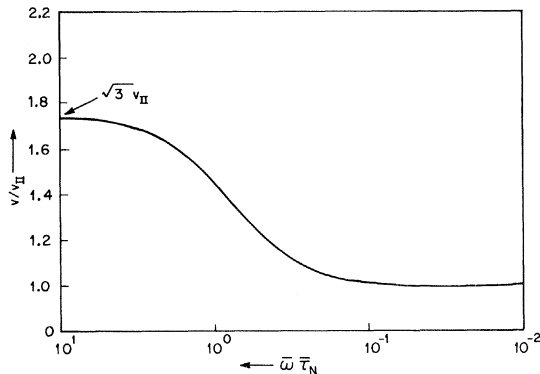


FIG. 1. Dispersion relation for heat-pulse velocity v as a function of $\bar{\omega}\bar{\tau}_N$ obtained using Eq. (2). v_{II} is the second-sound velocity and is reached only for very small $\bar{\omega}\bar{\tau}_N$.

given a satisfactory and simple description of the experimental data for solids, was that of Rogers.¹⁷ He used *hydrodynamic* equations and introduced a second viscosity which depended strongly of $\bar{\omega}\bar{\tau}_N$. Assuming plane-wave solutions for the temperature ($T = T_0 e^{i(kx - \omega t)}$), the heat-flow equation was solved and the resulting dispersion relation for the temperature wave was given by

$$k^2 v_{II}^2 = \frac{1}{3} k^2 v_1^2 = \omega^{-2} + \frac{i\bar{\omega}k^2\bar{\tau}_N(v_1^2 - v_{II}^2)}{1 - i\bar{\omega}\bar{\tau}_N}. \quad (2)$$

Here v_{II} is the second-sound velocity and v_1 is the ballistic velocity. In the above it was implicitly assumed that the single-particle-like excitations could be characterized by a single isotropic branch and that the ballistic velocity, corresponding to this single branch, had no dispersion of its own. In Fig. 1 we have plotted the real part of the phase velocity (ω/k) derived from (2) as a function of $\bar{\omega}\bar{\tau}_N$. It is clear that for small $\bar{\omega}\bar{\tau}_N$ one obtains the limiting second-sound velocity $v_{II}/\sqrt{3}$, while for large $\bar{\omega}\bar{\tau}_N$ one obtains the ballistic velocity v_1 as expected. There is considerable dispersion in the heat-pulse velocity for values of $\bar{\omega}\bar{\tau}_N \sim 1$. It is important to point out here that in Fig. 1 the values of $\bar{\omega}\bar{\tau}_N$ are plotted logarithmically. It is clear that the transition region is quite broad; it is necessary to span a range of about two orders of magnitude in $\bar{\omega}\bar{\tau}_N$ before the limiting behavior described above is obtained. Even though one has some latitude in varying $\bar{\omega}$, the chief quantity which can be changed is $\bar{\tau}_N$ through its temperature dependence. For typical variations of $\bar{\tau}_N$ as T^3 or T^4 it is clear that one requires, again, a rather large window in temperature for observing the full dispersion relation shown in Fig. 1. Experimentally, as we shall see later, one can get a truly short $\bar{\tau}_N$ only in the case of a gas of particles (where $\bar{\tau}_N$ can be varied at will) and in the roton-dominated region of He II where the density of excitations is sufficiently high at a convenient temperature. In other instances, one at best obtains an *approach* to the ideal behavior before other processes take over.

It is worth reemphasizing that (2) is derived in the hydrodynamic limit where the concept of second viscosity is valid. Hence there is reason to believe that the results are not strictly valid for the region approaching ballistic behavior, although the asymptotic limit $v = v_1$ is certainly correct.

2. Sound (heat-pulse) propagation in gas

Even though the propagation of low-frequency adiabatic sound has been well studied since the days of Laplace and Newton, it is only in the last decade or so that one has been able to obtain, by means of theoretical statistical mechanics, a detailed microscopic description of the formation of

the collective mode from the individual single-particle-like excitations, and hence the dispersion law for sound in a simple monotonic gas at high frequencies. This has been discussed recently in the theoretical articles by Wang-Chang and Uhlenbeck¹⁸ and by Foch and Ford¹⁹ who showed the connection between the approximate dispersion law for sound from hydrodynamics and the more rigorous calculations using the linearized Boltzmann equation and the collision-time approximation.

In a gas of interacting particles, both the hydrodynamic and the Boltzmann equation approach yields, when one looks for "sound-like" solutions, five normal modes to the eigenvalue problem. These five modes in turn arise because there are five independent constants of the motion: number of particles, three components of linear momentum, and the energy. Out of these five normal-mode solutions, it turns out that the dispersion relation for three of the modes yields imaginary frequencies ω for real values of the wave vector \vec{k} , i. e., they are nonpropagating modes which when excited damp monotonically in time toward equilibrium, at least in the long-wavelength limit when the solutions are accurate. Two of these nonpropagating modes involve mainly transverse-velocity motions (shear waves) while the third is the so-called heat-conduction mode which involves mainly fluctuations in the entropy. Finally, the remaining two modes are propagating modes (one going to the right and one to the left) and involve primarily fluctuations in the *number density* of particles and have mainly a longitudinal component of velocity. These *sound* modes have for very small k the linear-dispersion relation

$$\omega = \pm v_s^0 k \quad (3)$$

with the sound velocity at low frequencies being given by

$$\begin{aligned} v_s^0 &= (\gamma p / \rho)^{1/2} = (\gamma k T / m)^{1/2} \\ &= (\frac{1}{3} \gamma \bar{v}_1^2)^{1/2}, \end{aligned} \quad (4)$$

where p is the pressure, ρ the density, T the temperature, $\gamma = C_p / C_v = \frac{5}{3}$ for a monoatomic gas, and \bar{v}_1 is the average ballistic velocity of the particles obtained from the equipartition theorem ($\frac{1}{2} m \bar{v}_1^2 = \frac{3}{2} k T$).

It is important to reiterate here that in the elementary-excitation picture the sound mode involves a periodic fluctuation in the number density of the elementary excitations, in this case the particles themselves. The coherent sound mode is formed through the interaction among the particles in a well-defined way (conservation of energy and momentum, etc.) and turns out in the long-wavelength limit, at least, to be the only eigenvalue of the collision operator in the Boltzmann equation which

corresponds to a propagating mode. In this more general sense, the sound mode in a gas is analogous to the second-sound mode in the phonon gas. This is further evidenced by the fact that the relationship between the ballistic velocity of the elementary excitations (atoms or phonons) and the sound or second-sound velocity in the two cases is also similar. However, in the case of an atomic gas²⁰ the ratio is modified by the adiabatic compressibility factor γ which is unity for the phonon gas. We wish to emphasize this analogy since usually the sound mode in a gas is thought of as a pressure wave and not a temperature wave. This is because the generation of sound (by the usual means of tuning forks, piezoelectric transducers, etc.) and its detection (by means of a microphone or by the ear) is typically done by pressure-sensitive devices. However, variations in the density can be introduced by means of thermal generators and detectors as well, since in a gas the density is related to the pressure and temperature via the gas laws. Thus, heat pulses in gases may be expected to propagate as well-defined collective pulses (sound waves) with a velocity given by the dispersion relation as long as the dominant frequency in the pulse is not too large (small compared to the inverse collision time τ^{-1}).

The question may be asked, what happens as ω is made larger and larger. Experimentally, in conventional sound experiments, Greenspan²¹ has reached values of $\omega \tau \sim 1$ for several inert gases and in Fig. 2 we show from his work the reduced velocity v_s^0 / v_s and the attenuation $\alpha v_s^0 / \omega$ as a function of $\omega \tau$. The theoretical work of Wang-Chang and Uhlenbeck and Foch and Ford was in fact motivated originally by these experiments. Their theoretical calculations of the dispersion relation for sound at high frequencies using the Boltzmann equation may be summarized as follows. As ω is made higher and higher, the attenuation and velocity of the sound mode increases monotonically until a critical value ω_{cr} , when the discrete mode ceases to exist and merges with the continuum of single-particle modes. The existence of a critical frequency is believed to be a general phenomenon and is a consequence of the finiteness of the collision time τ . At sufficiently short wavelengths only the single-particle modes remain. The value of the critical frequency depends on the specifics of the model and the spectrum of relaxation times assumed. In Fig. 2 the dashed lines correspond to the numerical calculations of Foch and Ford¹⁹ using the Boltzmann equation for the dispersion and attenuation of the sound mode for values of $\omega \tau$ up to about 1. Since perturbative methods are used, the computations are believed to be most accurate for these small values of $\omega \tau$.

It is clear from the above brief discussion that

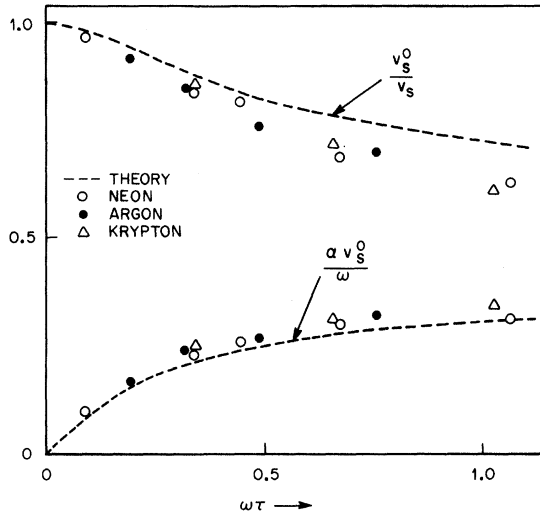


FIG. 2. Measured sound velocities v and attenuation α for several inert gases. After Greenspan (Ref. 21) v_s^0 is the low-frequency sound velocity. The dashed curves are obtained from the theory of Foch and Ford (Ref. 19).

a study of the dispersion of sound and the transition to ballistic flow in gases is of interest not only because of its close analogy to second sound in the phonon gas but also because such experiments are a critical test of the Boltzmann equation in statistical mechanics.

3. Heat pulses and velocity of second-sound in helium II

So far we have ignored the effect of dispersion in the elementary-excitation spectrum on the velocity of second sound in solids. However, since the early conjectures of Landau and subsequent verification by neutron measurements,²² it is known that the He II excitation spectrum is highly dispersive, particularly at energies greater than that of the roton minimum. In this section, we wish to explore the effects of dispersion of the velocity of second sound in He II.

As pointed out in Sec. I, Landau³ used two-fluid hydrodynamics and showed that the measured second-sound velocity in high temperatures could be explained through the existence of a gap in the excitation spectrum at a finite value of the wave vector \vec{k} . Many years later, Bendt, Cowan, and Yarnell²³ utilized the dispersion curves measured by neutron scattering to calculate the various thermodynamic quantities such as the entropy S , specific heat C , and the normal-fluid density ρ_n . Using Landau's expression (1) they calculated the temperature dependence of v_{II} and obtained good agreement with existing experimental data. However, the reliance on calculations based on thermodynamic quantities precluded a detailed microscopic un-

derstanding of second sound in He II, particularly with regard to the contributions of the various branches of the spectrum at temperatures below 1 K.

In order to get a clearer physical understanding of the velocity of second sound in He II, we apply the Boltzmann equation to a gas of excitations possessing dispersion. We assume, initially, that there is strong scattering among all the excitations of the system (hydrodynamic regime $\omega\tau \ll 1$) and that the perturbations from ambient are small. Kwok,²⁴ for the case of solids, showed that under the above conditions the Boltzmann equation can be solved and the velocity of second sound v_{II} is given by

$$v_{II}^2 = \frac{1}{3} \left(\sum_k \omega_k S_k^0 \vec{k} \cdot \vec{u}_k \right)^2 \left(\sum_k S_k^0 \omega_k^2 \right)^{-1} \times \left(\sum_k S_k^0 k^2 \right)^{-1}. \quad (5)$$

In (5), $S_k^0 = N_k^0 / (N_k^0 + 1)$, where N_k^0 is the equilibrium Bose-Einstein distribution function, and \vec{u}_k is the elementary-excitation group velocity $\nabla_k \omega_k$. It is easy to show that (5) yields the correct value of v_{II} in the case of linear-phonon-dispersion curves, i. e., if $\omega_k = vk$,

$$v_{II}^2 = \frac{1}{3} \left(\sum_k S_k^0 \omega_k^0 \right) \left(\sum_k S_k^0 k^2 \right)^{-1} = \frac{1}{3} \frac{\omega^2}{k^2} = \frac{1}{3} v^2, \quad (6)$$

as expected. It is clear from (5) that in the presence of dispersion, v_{II} will be a function of T because the Bose-Einstein occupation numbers for different parts of the excitation spectrum will change as T is varied. In Fig. 3 we show the results of a numerical evaluation of expression (5) using the experimental dispersion curve determined by inelastic neutron scattering^{25,26} at 1.1 K for SVP and for 24 bar. For temperatures below about 1.4 K these computed curves are in excellent agreement with computations based on the thermodynamic quantities [expression (1)]. We have not taken into account any temperature dependence of the $\omega-k$ curve so that the calculations are most reliable around 1.1 K. We have also not tried to use different "best fits" to the neutron data.²⁷ They are expected to make small differences to the curves shown in Fig. 3. Finally, at high temperatures greater than ~ 1.4 K the elementary-excitation picture in helium II becomes less applicable as the excitations broaden considerably with increasing temperature and become ill defined. Near T_λ , as this picture of elementary excitations is no longer even approximately correct, one has to go back to the thermodynamic expression to get the correct second-sound velocity.

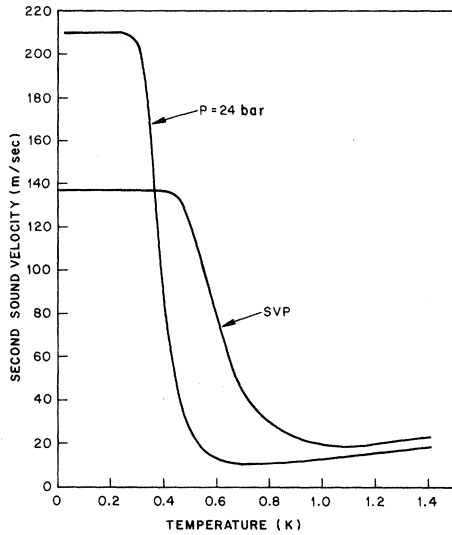


FIG. 3. Computed second-sound velocity as a function of temperature for SVP and 24 bars. Equation (6) was used to calculate these curves. See text.

The fact that an elementary-excitation picture would break down as one approaches T_λ was also pointed out by Dingle.²⁸ In a rather different description of second sound in terms of the elementary excitation it was argued that the elementary-excitation picture was only valid where the effective mass of the normal-fluid density ρ_n was small relative to the inertial mass.

We would, nevertheless, like to emphasize that the elementary-excitation picture gives a very good physical description of the absolute velocity and temperature dependence of second sound in helium II. In this picture, the low second-sound velocity at high temperature arises as a result of the combined effect of the large density of roton states of low group velocity and the near cancellation of the contributions from either side of the dispersion curve about the roton minimum due to the $\vec{k} \cdot \vec{u}_k$ term in (5). On the low- k side of the roton minimum the heat current, which is determined by the group velocity, and the momentum lie in opposite directions, and $\vec{k} \cdot \vec{u}_k$ is negative. This cancellation is not exact because the roton minimum is located at a finite value of k and the summation over k contributes more phase space for the positive $\vec{k} \cdot \vec{u}_k$ components.

The effect of the rotons is most clearly illustrated by comparing the second-sound velocity curves shown in Fig. 3 for low and high pressures. Since the effect of pressure is to increase the sound velocity but decrease the roton gap, the persistence of low-velocity second sound to lower temperatures at higher pressures indicates that the rotons dominate the phonons in determining the second-sound velocity as long as they are populated

in significant numbers. These concepts are elucidated further when one looks at only the roton contribution to the second-sound velocity and assumes that the phonon-roton gases are decoupled from each other (a situation which we shall see later is experimentally achievable at high pressures). The computed velocity of roton second sound as a function of temperature at a pressure of 24 bar is shown in Fig. 4. With increasing temperature this velocity increases monotonically from zero, at first linearly, as higher-velocity roton excitations are thermally populated. The effect of the negative velocity branch is also illustrated in Fig. 4 where we plot the expected second-sound velocity from roton excitations involving the positive branch alone. This velocity is now considerably higher than that for roton second sound consisting of both branches.

In summary, it is clear that the elementary-excitation picture gives a physically appealing description of second sound in He II over a wide range of temperature. It illustrates also the profound influence of the shape of the ω - k curve on the velocity of second sound, particularly when contrasted with the simple $1/\sqrt{3}$ times the ballistic velocity expression obtained for a dispersionless excitation spectrum.

4. Solids

In earlier sections several general remarks were made on the relationship and analogy of second sound in a phonon gas and sound in a gas of particles. We have also seen the effect of a finite collision time, which causes a transition to ballistic single-particle-like excitations at high frequen-

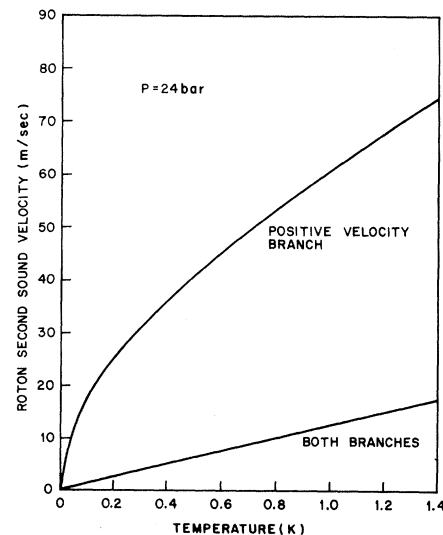


FIG. 4. Computed roton second-sound velocity as a function of T ; $P = 24$ bars.

cies. In this section we wish to highlight the consequences of two effects which are peculiar to the case of the phonon gas in solids: (i) the fact that the solid is really a multiple-polarization system; and (ii) the fact that the collisions between the phonons are not necessarily momentum conserving.

For a multiple-polarization system in the Debye approximation $\vec{u}_\lambda = u_\lambda(\vec{k}/|k|)$, where λ is the branch index, the second-sound velocity is given by^{29,30}

$$v_{II}^2 = \frac{1}{3}(C_3/C_5), \quad (7)$$

where

$$C_n = \sum_\lambda \frac{1}{u_\lambda^n} \quad (8)$$

In (7) it is assumed that thermodynamic equilibrium between the different polarization branches is achieved. If this is not realized, one might expect "second sound" in the individual branches. Furthermore, in the Debye approximation each polarization λ is represented by a particular velocity u_λ which is assumed isotropic. In reality, in materials such as solid He and bismuth, the individual polarizations have velocities which are highly anisotropic. It is possible, in principle, to take this into account by constructing the group-velocity surface as a function of angle and summing up over all the modes using an expression such as (5). However, if mode mixing does indeed occur in the formation of second sound, it seems reasonable to assume that an appropriate average ballistic velocity will be given by the Debye velocity v_D where

$$v_D \simeq (k_B/\hbar) \Theta_D (6\pi^2 N/V)^{-1/3} \quad (9)$$

is calculated from the measured Debye temperature Θ_D in the temperature range of interest, the number of atoms of per unit cell, N , and the atomic volume V . Under the assumption that the Debye average represents an appropriate thermodynamic average of the different polarization modes, we obtain

$$v_{II} = v_D/\sqrt{3}. \quad (10)$$

We shall see that this is approximately borne out by our experiments.

We now turn to the question about the importance of resistive processes. As is well known, resistive processes in solids cause rapid degradation of second sound in the phonon gas. The condition for the observation of *unattenuated* second sound is the well-known frequency window discussed at length by Krumhansl, Prohofsky, and Guyer,^{5,6}

$$\bar{\omega} \bar{\tau}_N \ll 1 \ll \bar{\omega} \bar{\tau}_R. \quad (11)$$

In (11), $\bar{\tau}_N$ and $\bar{\tau}_R$ are the momentum-conserving and -nonconserving mean relaxation times, respectively. The velocity of this unattenuated sec-

ond sound has a limiting value v_{II} discussed earlier. If, however, we allow for finite values of $\bar{\tau}_R$ and hence attenuation, it is possible for second sound to exist for a range of values of $\bar{\tau}_R$ before heat propagation becomes entirely diffusive. This question has been examined theoretically in the very recent papers of Ranninger³¹ and of Beck and Beck.³² Assuming a mean relaxation time $\bar{\tau}$, using the usual expression $\bar{\tau}^{-1} = \bar{\tau}_N^{-1} + \bar{\tau}_R^{-1}$, they show that second sound can propagate as long as $\bar{\omega} \bar{\tau} \lesssim 1$ and $\bar{\omega} \bar{\tau} \gtrsim 1$, thus relaxing (11) somewhat. The velocity of this "attenuated" second sound, v'_{II} , in the presence of resistive processes turns out to be a decreasing function of $1/\tau_R$ and has a value approximately given by

$$v'_{II} = v_{II}/(1 + 2\alpha)^{1/2}, \quad (12)$$

where

$$\alpha = (1 + \bar{\tau}_R/\bar{\tau}_N)^{-1}. \quad (13)$$

Beck and Beck³² have shown that (12) is approximately valid as long as $\bar{\omega} \bar{\tau}_R > 2$. For values of $\bar{\omega} \bar{\tau}_R$ approaching 2, they show that v_{II} approaches zero, and heat propagates mainly by diffusion.

B. Lifetimes of elementary excitations in He II

In Sec. II A 3 we gave an expression for the velocity of second sound in helium II based on the assumption that the lifetimes of the excitations, namely, phonon-phonon scattering time (τ_{pp}), phonon-roton scattering time (τ_{pr}), and roton-roton scattering time (τ_{rr}) were all short (relative to the propagation time and pulse duration) so that second sound in the entire gas of excitations was a well-defined mode of the system. Thus, the temperature dependence of the second-sound velocity (Fig. 3) arose solely from the variations in the thermal population of different branches with temperature. We now wish to consider the possibility of additional variations in the heat-pulse velocity due to finite-relaxation-time effects, and we summarize below what is known about τ_{rr} , τ_{pr} , and τ_{pp} from existing theories and previous measurements.

1. Roton-roton scattering

The scattering of two rotons into two other rotons was first considered by Landau and Khalatnikov.^{33,34} They assumed that the potential of interaction between the colliding rotons had a δ -type character [$V = V_0 \delta(r)$ and r is the relative distance between the pair of colliding rotons]. Using the laws of conservation of energy and momentum and assuming a parabolic form for the roton-excitation spectrum (valid for rotons *near* the *minimum*) they integrated the matrix element over the phase space of the scattered rotons and showed that

$$1/\tau_{rr} = (4p_0\mu |V_0|^2/\hbar^4) N_r. \quad (14)$$

Here N_r is the roton number density which varies as $T^{1/2} e^{-\Delta/kT}$, where Δ is the roton energy at the minimum, p_0 is the momentum at the roton minimum, and μ the roton effective mass. From viscosity and Raman-scattering measurements,³⁴ $|V_0|^2$ is found to be $\sim 4 \times 10^{-76}$ erg cm⁻³. Because of the exponential dependence of N_r on the ratio Δ/kT , we find that $1/\tau_{rr} \sim 3 \times 10^6$ sec⁻¹ for $T \sim 0.6$ K at SVP and for $T \sim 0.5$ K at 24 bar. Thus once the rotors are thermally excited in sufficient numbers ($N_r \sim 10^{16}$ cm⁻³), their lifetime due to collisions is always short enough to cause equilibrium in the roton gas of excitations for heat-pulse experiments of the type reported here.

We wish to reemphasize that the above estimate and the more sophisticated recent ones by Yau and Stephen³⁵ and by Solana *et al.*³⁶ are valid for excitations about the roton minimum. These scattering cross sections can be severely modified for higher-energy roton excitations away from p_0 . From neutron measurements at SVP³⁷ it is known that over a small region beyond the roton minimum the dispersion curve is linear with a group velocity approaching the sound velocity. These "fast" rotors can decay by phonon emission. This decay rate has recently been calculated by Jäckle and Kehr³⁸ and the zero-temperature limiting value of this decay rate $\sim 3 \times 10^8$ sec⁻¹. In Sec. II B 2 we consider in detail the phonon lifetime due to interactions with rotors.

2. Phonon-roton scattering

The laws of conservation of energy and momentum require that the phonon-roton scattering be a four-particle process of the type $P_1 + R_1 \rightleftharpoons P_2 + R_2$. Since the momentum of the phonon is much smaller than the momentum of the roton, the scattering involves almost no change in the direction of the roton momentum and little change in the magnitude of the phonon momentum. The matrix element for the scattering consists of two main terms: (a) a deformation-potential-type interaction which arises from the density variation of the phonon field which can be related to the density variation of the roton energy; and (b) a $\vec{v}_{ph} \cdot \vec{P}_R$ type of interaction which arises from the velocity variations of the phonon field \vec{v}_{ph} (*v. t.*).

The expression for the relaxation rate τ_{PR}^{-1} due to the above-mentioned scattering processes has been given by Khalatnikov and Chernikova³⁹ who show that

$$\tau_{PR}^{-1} = (2\pi)^{1/2} \Gamma(k_B^{9/2}/h^7) \times \left(\frac{p_0^4 \mu^{1/2}}{\rho^2 v_{ph}^5} \right) T^{9/2} e^{-\Delta/k_B T}, \quad (15)$$

where ρ is the density,

$$\Gamma = \frac{2}{9} + \frac{1}{25} (p_0/\mu v_{ph})^2 + \frac{2}{9} (p_0/\mu v_{ph}) A + A^2 \quad (15a)$$

and

$$A = \left(\frac{\rho^2}{p_0 v_{ph}} \right) \frac{\partial^2 \Delta}{\partial \rho^2} + \left(\frac{p_0}{\mu v_{ph}} \right) \left(\frac{\rho}{p_0} \frac{\partial p_0}{\partial \rho} \right)^2. \quad (15b)$$

The explicit forms of (15), (15a), and (15b) are the same as that given by Abraham *et al.*⁴⁰ The first two terms in (15a) arise from the velocity-field term and the latter two from the density variations. These latter terms are small because of the weak dependence of Δ on ρ and p_0 on ρ so that the value of $A \approx -0.1$, while the value of $p_0/\mu v_{ph} \approx 8$. Thus the dominant contribution to τ_{PR}^{-1} comes from the second term in Γ . Thus, neglecting the small variations in (15) due to the dependence of μ , ρ , and p_0 on the pressure, it is clear that the primary effect of pressure on τ_{PR}^{-1} will be due to the approximate v_{ph}^{-7} dependence on the phonon velocity and the exponential dependence on the roton gap Δ/kT . It turns out that these two terms nearly cancel, so that τ_{PR}^{-1} is relatively insensitive to pressure. Numerically τ_{PR}^{-1} is of the order of 10^5 sec⁻¹ at about 0.6 K so that phonon-roton scattering is expected to be important in our experiments at intermediate temperatures.

The discussion of phonon-roton scattering is valid for the parabolic region of the roton-dispersion curve. As mentioned in (a) in the "linear" region of the roton-excitation-curve absorption of phonons by "fast" rotors is possible. This process has been discussed in the paper by Jäckle and Kehr³⁸ and the reader is referred to their paper for details.

3. Phonon-phonon scattering

A knowledge of the lifetimes of thermal phonons in liquid helium II, at temperatures below the roton-dominated region, is of considerable general interest. A detailed knowledge of the phonon-phonon collisions in He II could shed light on the more difficult problem of phonon lifetimes in dielectric solids, since liquid helium has only a single isotropic phonon branch and is free of dislocations and impurities. Ever since the earliest calculation of Landau and Khalatnikov,³³ numerous attempts to calculate the phonon-phonon scattering time τ_{pp} have been made. In this section we briefly review these calculations and discuss the consequences for the propagation of heat pulses in the phonon-dominated region of He II.

Since the collisions between the phonons must satisfy energy and momentum conservation, the lifetime τ_{pp} depends sensitively on the nature of the dispersion relation for the relevant phonons. For energies below a few degrees kelvin the dispersion relation most commonly assumed has the

form

$$\epsilon = v_{ph}^0 p(1 - \gamma p^2 \dots). \quad (16)$$

Here v_{ph}^0 is the phonon velocity for momenta $p=0$ and γ is a dispersion parameter. For dispersionless phonons ($\gamma=0$), energy and momentum conservation allows only *collinear* three-phonon processes ($p_1 = p_2 + p_3$). On the other hand, for "normal" dispersion, ($\gamma > 0$) Pethick and Ter Haar⁴¹ show that the three-phonon process is allowed only if one takes into account the energy uncertainty in the excitation spectrum due to the finite lifetime itself. For "anomalous" dispersion ($\gamma < 0$) the three-phonon process is allowed and involves the interactions of nearly collinear phonons with transverse momentum also conserved. The angle of scattering is determined by the amount of anomalous dispersion and the momentum (frequency) of the phonons in question. Since the value of γ is small, this type of scattering is always a small-angle scattering process and hereafter will be distinguished by a superscript (") to distinguish it from the wide-angle scattering rates to be discussed later.

Numerically, the parallel three-phonon process for dispersionless phonons has been shown by Jäckle⁴² to have the value

$$\tau_{pp}''(3, \gamma=0) \approx 2.5 \times 10^{-10} T^{-5} \text{ sec} \quad (17)$$

at SVP. Thus $\tau_{pp}''(3, \gamma=0)$ has a value of 2.5×10^{-5} sec at 0.1 °K and $\sim 10^{-8}$ sec at 0.5 °K. According to Jäckle, $\tau_{pp}''(3, \gamma=0)$ depends on the phonon velocity as V_{ph}^5 and on the Grüneisen parameter μ as $(u+1)^{-2}$, so that it turns out that the effect of pressure is to increase the relaxation time. At 24 bar we find that this increase is about an order of magnitude from that given by Eq. (17).

Maris⁴³ has calculated the value for τ_{pp}'' for $\gamma < 0$. At SVP his numerical value for the three-phonon process, assuming anomalous dispersion, is almost identical to the value obtained by Jäckle for dispersionless phonons. At higher pressures, though, the lifetime $\tau_{pp}''(3, \gamma < 0)$ changes drastically as has been shown by Jäckle and Kehr.⁴⁴ They took into account additional higher-order terms in the expansion (16) for the dispersion relation. At large momenta these higher-order terms cause the dispersion to become normal and hence they introduce a cutoff in the three-phonon process. They assume that the cutoff momentum⁴⁵ depends strongly on pressure in order to explain the ultrasonic-attenuation data⁴⁶ under pressure. Thus their calculations show that the three-phonon process ceases to be effective at high pressures and the reader is referred to their paper for numerical estimates of the parallel process rate with anomalous dispersion as a function of pressure.

It is important to emphasize that in all of the

above calculations the effect of the broadening of the excitation spectrum due to the finite lifetime is not taken into account self-consistently. Thus the calculations can be severely affected not only by the choice of γ but also by the finiteness of the lifetime itself. The possibility of solving the generalized Boltzmann equation at finite temperature *self-consistently* has been discussed by Meier and Beck⁴⁷ but we know of no numerical results. The importance of *finite* temperatures on the dispersion parameter γ has also not been taken into account.

In the discussions so far we have restricted ourselves to three-phonon processes only. The four-phonon process, which occurs for all form of the dispersion relation, was first considered by Landau and Khalatnikov³³ and later by Khalatnikov and Chernikova.³⁹ The four-phonon-process matrix elements consist of two parts: (i) an almost collinear interaction and (ii) a wide-angle process involving the scattering of two phonons into two other ones. The small-angle form of the phonon-scattering time $\tau_{pp}''(4, \gamma > 0)$ has been shown by Eckstein⁴⁸ to have the numerical value at SVP,

$$\tau_{pp}''(4, \gamma > 0) \approx 11 \times 10^{-45} \gamma T^{-7} \text{ sec.} \quad (18)$$

Here again the parallel-process rate depends on the value of the dispersion parameter γ . With increasing γ (increasing pressure) the lifetime increases. The lifetime for the wide-angle four-phonon process has also been calculated by Khalatnikov and Chernikova. They give

$$\tau_{pp}''(4, \gamma > 0) \approx \frac{2^{13}}{9 \times (13)!} \frac{h^7 (\rho v_{ph}^5)^2}{(u+1)^4} (k_B T)^{-9} \quad (19)$$

for $T=0.5$ K, $\tau_{pp}''(4, \gamma > 0)$ has a value of about 1.7×10^{-5} sec for SVP. This time increases markedly with pressure because of the v_{ph}^{10} dependence of the relaxation time on the phonon velocity.

The calculations of the four-phonon process have all been performed for $\gamma > 0$ only. These processes could conceivably have a widely different temperature and pressure dependence for $\gamma < 0$.

We now turn to the implication of the relaxation times discussed above for our heat-pulse experiments. Since τ_{pp}'' involves nearly collinear-scattering processes, the parallel-process relaxation cannot be the relevant time in determining the transition from ballistic to fully developed second sound in the phonon gas. Even in the presence of strong τ_{pp}'' one has to allow for considerable angular spread to cause equilibration of perpendicularly moving phonons. For $\gamma \sim -8 \times 10^{37}$ cgs units, Maris⁴⁹ estimates that the scattering angle in the small-angle three-phonon process is of the order of a few degrees. Thus numerous small-angle collisions are required to cause a direction change of 90°. Of course, the wide-angle four-phonon process $\tau_{pp}^1(4,$

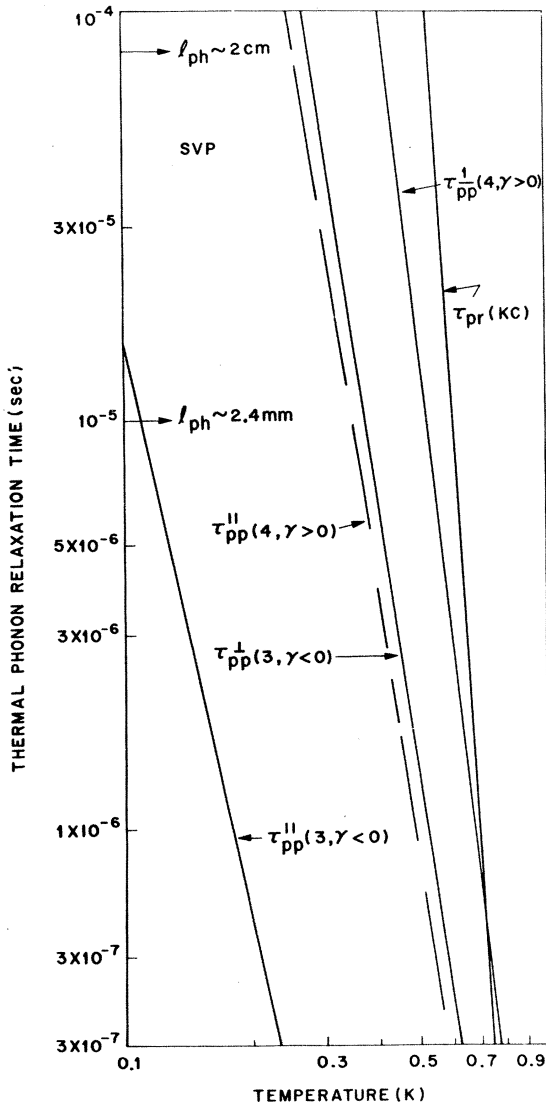


FIG. 5. Calculated thermal-phonon relaxation times as a function of temperature at SVP. The superscript double prime refers to small-angle scattering while \perp to large-angle scattering. $\gamma < 0$ means anomalous dispersion. The three- and four-phonon process rates were calculated from Eqs. (17)–(19). $\tau_{pr}(KC)$ using Eq. (15) (see text). The mean free paths at our sample lengths of 2.4 mm and 2 cm are also indicated.

$\gamma > 0$) of Landau and Khalatnikov can give rise to equilibration in the phonon gas directly. Thus our *heat-pulse* experiment will yield a measurement of a *wide-angle* scattering time. It is not necessarily the case, however, that the value obtained in this type of measurement is a measure of τ_{pp}^{\perp} as defined in (19). If $\tau_{pp}^{\prime\prime}$ is sufficiently short, relative to τ_{pp}^{\perp} , then many almost collinear-scattering processes could result in an *effective* $\tau_{pp}^{\perp}(\text{eff})$. Maris⁴⁹ has studied this effect in some detail and numerical estimates are given below which may or may not

be related to the small-angle scattering time $\tau_{pp}^{\prime\prime}$. For a direct measurement of the small-angle time, experiments with monochromatic sound waves are necessary.⁵⁰ These will be reported in a subsequent paper. It is clear though, that both sets of measurements are required to get a complete picture about the lifetimes of phonon excitations in liquid helium.

In Fig. 5 we have plotted the different relaxation times calculated for thermal phonons as a function of the ambient temperature T at SVP. We have indicated by arrows the relaxation time at which the mean free path $v_{ph} \tau_{pp}$ is equal to our sample lengths of 2.4 mm and 2 cm. In the model of Khalatnikov and Chernikova³⁹ both $\tau_{pp}^{\prime\prime}$ and τ_{pp}^{\perp} are sufficiently long (below about 0.25 K for the long cell) so that the propagation is truly ballistic at low temperatures. Phonon-roton interactions become important only around 0.55 K and dominate above 0.72 K. On the other hand, in the work of Maris⁴⁹ and Jackle and Kehr,⁴⁴ $\tau_{pp}^{\prime\prime}$ for three-phonon processes is very short except at the lowest temperatures. In their model heat pulses are described by a “pseudo”-ballistic pulse (excepting perhaps in our short cell below 0.12 K). Their $\tau_{pp}^{\perp}(\text{eff})$ is also considerably shorter than that of Khalatnikov and Chernikova and has significant effects on heat pulse propagation at $T \sim 0.28$ K for the long cell and 0.36 K for the short cell. Their theoretical temperature dependence at low temperatures for $\tau_{pp}^{\perp}(3, \gamma < 0)$ is, however, stronger than the T^5 dependence for $\tau_{pp}^{\prime\prime}$ because the perpendicular-process rate in their model depends on the fourth power of the angle in the small-angle scattering. This angle depends on the temperature approximately linearly and so at $T \lesssim 0.1$ K the $\tau_{pp}^{\perp}(\text{eff})$ is expected to behave like T^{-9} . Maris argues, however, that as T is raised, the higher-frequency excitations are not subject to the $3pp$ and hence the strong T^{-9} dependence is substantially reduced.

We have not shown the effect of pressure on the relaxation rates in Fig. 5. But suffice it to say that τ_{pr} remains virtually unchanged, but that $\tau_{pp}^{\prime\prime}$ and $\tau_{pp}^{\perp}(\text{eff})$ are both expected to increase (for the same temperature) markedly with increasing pressure. Above about 10 bar and below about 0.5 K τ_{pp} is expected to be long in all models and the propagation should consist of true ballistic-phonon components.

III. EXPERIMENTAL TECHNIQUES

Many of the experimental techniques used in this work have been discussed in the past.⁹ In this section, we give only some of the salient features which we believe will be particularly helpful to the reader.

The helium experiments were done with a He³-He⁴ dilution refrigerator built by S. H. E. Corpora-

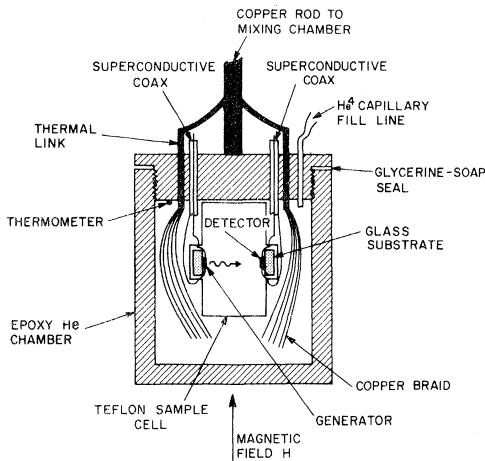


FIG. 6. Schematic of sample chamber used in liquid-helium experiments. The geometry of the generator and detector is that appropriate for the short cell. The long-cell experiments were done in a vertical geometry.

ation. The refrigerator had three sintered-foil heat exchangers in addition to a continuous exchanger and had a cooling capacity at 0.1 K of about 250 erg/sec. The mixing chamber was made of copper with provision for internal access. Under continuous operation, the refrigerator could reach an ultimate temperature of about 14.7 mK measured by a CMN thermometer attached to the mixing chamber.

The experimental helium chamber was attached to the mixing chamber by means of a copper rod soldered to its bottom. A schematic of this chamber, which was made out of epoxy, is shown in Fig. 6. The chamber was detachable by means of a threaded joint which was sealed at the beginning of each run by means of glycerine-soap solution. Two different size chambers were used. One had an internal diameter of $\frac{15}{16}$ in. and was 1 in. long while the other was also of the same diameter but had a length of $3\frac{1}{2}$ in. The chambers, filled with helium, could be cooled to 0.1 K within 1–2 h after starting the refrigerator. The cooling of the helium was achieved by means of hundreds of fine copper wires which were in the form of a bundle soldered to the copper rod. The temperature was measured by means of a carbon thermometer, previously calibrated against CMN, immersed in the liquid. Pressure was applied by means of a Hoke high-pressure regulator via the fill capillary and the experiments were always done under constant pressure. The pressure was measured by means of a Heise gauge whose calibration was checked with the known solidification pressure of helium.

The generator and detector were mounted opposite each other inside a Teflon holder with open sides. The separation L between the generator

and detector could be varied by means of Teflon spacers. Experiments were done for three different propagation lengths ($l \sim 0.25, 2.0, \text{ and } 7.0$ cm). The 0.25-cm length experiments were done in the horizontal geometry shown in Fig. 6 with the nearest walls being about 1 cm or more away from the centers of the generator and detector. Thus the short cell was entirely free of wall reflections. The experiments with the two longer lengths were done in a vertical geometry, and the Teflon spacers were separated to minimize the detection of pulses due to reflection at the walls. However, the presence of Teflon tape (used for electrical insulation purposes) around the open ends of the cells, could have given rise to some wall-scattered heat pulses at the detector in the case of the two larger length cells. The lengths themselves were accurately determined through the measurements of the arrival times of the echoes of the second-sound pulses at high temperatures. From the known second-sound velocity the length was determined and used for later determination of the heat-pulse velocities in the ballistic and transition regions.

The heat pulses were generated with a 50- Ω constantan heater film, $\sim 500\text{-\AA}$ thick, and were detected with a similarly deposited thin-film indium bolometer. The bolometer was magnetically biased at the midpoint of its resistive transition and then biased with a constant-current source. The precise mechanism through which the bolometer responds to thermal energy was not clear. Measurements of the dc temperature coefficient of resistance revealed that in the presence of the desired magnetic field the bolometer changed its resistance significantly ($\Delta R/R \sim 10^{-2} - 10^{-3}$) only at temperatures of the order of 0.5 K and above. It is possible that the biasing current and the heat pulse "primed" the thin-film bolometer sufficiently to bring it into its temperature-sensitive region. However, the detected voltage pulses were observed to scale with the bias current (for low bias current $\lesssim 100 \mu\text{A}$) indicating that there was no well-defined threshold and that dc heating was not significant. The sensitivity of the bolometer to heat pulses was found to increase when the temperature was raised to near T_c (at $H=0$) but even at very low temperatures our bolometers could detect voltage signals of the order of a few microvolts (energy flux $\sim 1 \text{ erg/cm}^2$ at the heater approximately 2.5 mm away from the bolometer with a signal-to-noise ratio in the ballistic region $\sim 10-1$). The possibility that at low temperatures some of the detection occurs through the movement of flux lines in the bolometer cannot be ruled out. From measurements with superconducting-tunnel-junction detectors⁵⁰ under the influence of magnetic fields of varying strengths, it appears certain that

our bolometers acted as true *broad-band* detectors of thermal energy in contrast to the quantum nature of the detection process of the junctions.

The sizes of the heaters and bolometers used in this work were typically 3.5×3.5 -mm square. The cryostat was equipped with superconducting coaxial cable to minimize losses down the cable. The voltage signals from the bolometer were amplified and fed into a Biomation 8100 transient recorder (with 10-nsec resolution) and accumulated in a multichannel analyzer. In some of the earlier data the signal averaging was done with a PAR 160 box car integrator. The current pulses to the constant heater were supplied by a Hewlett Packard 214A pulse generator. The pulse widths typically ranged from 0.1 to 1.0 μsec and the pulse amplitudes were usually ~ 0.5 – 5 V. Only rarely were higher amplitudes and pulse widths tried. Higher amplitudes and pulse widths resulted in distortion of the pulse shapes at the detector, as we shall see later. Most of the gas experiments were done in a manner described previously.⁹ These earlier experiments were done in the vapor which was in equilibrium with a small puddle of liquid at the bottom of the sample chamber and condensed film on all surfaces. The vapor pressure was varied by changing the ambient temperature of the sample chamber. In order to avoid varying the temperature, some more recent experiments were done above the liquefaction point (>4.2 K), and the mean free path was varied by changing the gas pressure. Because of the higher temperature of these experiments, a lead bolometer ($T_c \sim 7.2$ K in zero field) was used.

The bismuth samples used in our experiments were grown here at Bell Laboratories many years ago for electron-wave experiments and were known to have long electron mean free paths. As pointed out in our earlier paper,⁸ the crystals were handled with great care to avoid strain. The heaters and bolometers were electrically insulated from the bismuth by thin films of Ge and silicon oxide. Great care had also to be taken to avoid the breakdown of these insulating layers as electrical continuity to the bismuth from either heater or bolometer resulted in failure.

IV. EXPERIMENTAL RESULTS AND DISCUSSION

In this section we present our experimental results for the three experiments described in this work (gas, solid, and liquid). We first show and review our results in gaseous He^4 . We then present results on the transition to second sound in the phonon gas in crystalline bismuth. Finally our results on liquid He^4 are presented and analyzed.

A. Gaseous helium

We have previously⁹ reported on the velocity spectrum of evaporating atoms from a liquid-helium

surface at very low temperatures. We also presented some data which illustrated mean free path effects and showed the transition to adiabatic sound as the temperature and hence the vapor pressure was raised. At the low temperature of the earlier experiments the data in the ballistic and transition regions were found to be strongly amplitude dependent. In this section we present some heat-pulse data at a considerably higher temperature (~ 4.2 K) as a function of He^4 gas pressure and in a region where the heat-pulse temperature perturbation is small compared to ambient. These data then provide quantitative information on the number of collisions required for the formation of the collective mode from the single-particle excitations at MHz frequencies.

Some typical heat-pulse data as a function of vapor pressure are shown in Fig. 7 for $T \approx 4.2$ K. The input pulse width was about 0.8 μsec . For heater powers densities up to about 0.025 W/mm², the data showed no detectable variation. The vapor pressure at low temperatures was calculated through measurements of pressure at room temperature of known quantities of the gas. At the lowest pressure ($< 10^{-5}$ Torr) the detected heat pulse is extremely broad. In this region of pressure we are in the ballistic particle regime and what is

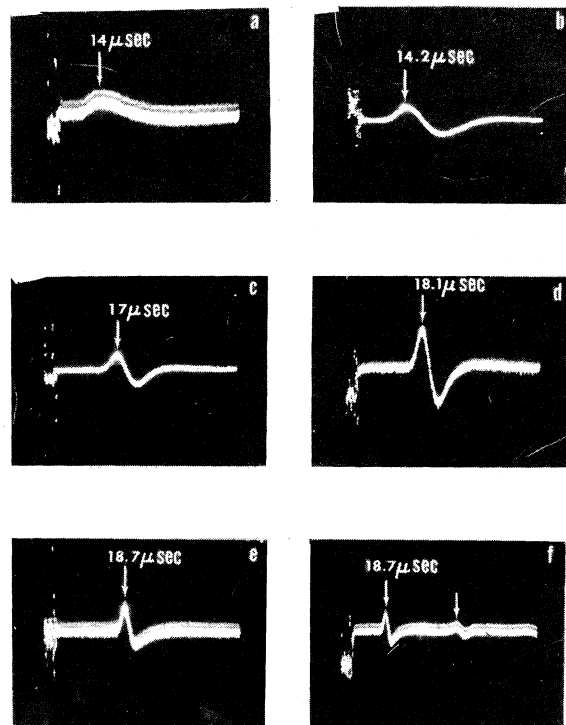


FIG. 7. Typical heat pulses in gaseous helium as a function of vapor pressure (in mtorr): (a) $< 10^{-1}$; (b) 0.5; (c) 30; (d) 70; (e) 400; (f) 400. Propagation length, 2.25 mm; $T = 4.2$ K.

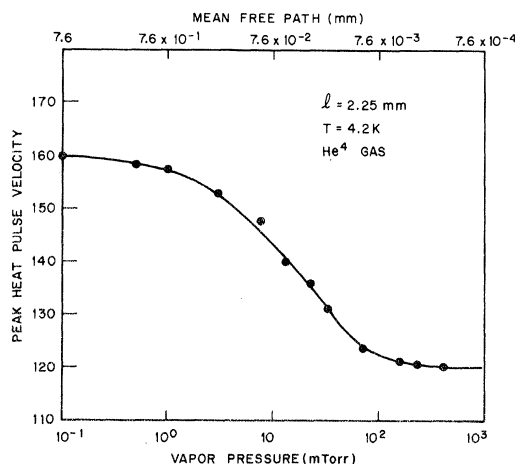


FIG. 8. Peak heat-pulse velocity as a function of vapor pressure; $T = 4.2$ K, $l = 2.25$ mm. Calculated mean free paths are also indicated.

measured is the velocity distribution reflecting the ambient temperature. As the pressure is raised beyond about 1μ the pulse begins to rapidly retard in time and also sharpen in time space. By about 30μ it develops an echo. At higher pressures one sees well-defined pulses as is clear from Fig. 7.

It is interesting to point out that well into this collective or temperature-wave regime, the detected pulse shape takes on more of a derivative form of the initial pulse. This has been discussed by Guernsey *et al.*⁵¹ and is due to the inductive nature of the temperature wave for our geometry. As we shall see later, very similar shapes are also observed in the second sound or temperature-wave regime in liquid He II.

The qualitative velocity behavior described above is shown as a quantitative velocity-profile plot in Fig 8. Saturation in the velocity at both the low- and the high-pressure ends is clear. These data, then, provide a quantitative description of the transition from ballistic single-particle flow to collective sound. From kinetic theory we can estimate the mean free path λ of the gas molecules as a function of pressure. The calculated values are shown at the top of Fig. 8. For a propagation length of $l \approx 2.25$ mm, it is clear that $\lambda \approx 1$ mm already has a significant effect on the velocity of the heat pulse. For $\lambda \sim 0.1$ mm one begins to approach a limiting behavior in the high-pressure region. It is also about the pressure region where one begins to see the development of the wave-like nature of the excitation through the observation of an echo. It appears, then, that under the conditions of our experiment one can say that some 50 collisions are required for the formation of the collective mode. We wish to emphasize that this depends somewhat on one's definition of sound. The transition region

is quite broad and is almost certainly due in part to the rather broad velocity distribution of the gas molecules. Truly, unattenuated sound formation occurs only in the presence of numerous collisions at elevated pressures. It is also clear from Fig. 8 that $v_s \sim [\frac{1}{3}\gamma(\bar{v}_1^2)]^{1/2}$ as expected from Eq. (4). This collective mode in the gas of particles which we call sound is then analogous to the collective mode in a gas of phonons or phonons and rotons which we call second sound.

The above measurements by the heat-pulse technique, in addition to being of considerable relevance to second-sound measurements, also complement the earlier data of Greenspan²¹ and Meyer and Sessler^{52,53} on the dispersion of sound using conventional piezoelectric transducers. From the observed length dependence of the phase velocity of the ultrasonic waves they concluded that some 15 collisions were required for the formation of sound. Our measurements, well into the Knudsen region, are made possible through the combined use of low-temperature techniques and highly sensitive superconductive bolometers. Sine wave measurements as a function of frequency and length should enable one to probe in great detail the transition from the ballistic Knudsen modes to the hydrodynamic collective mode. Our present pulse measurements, however, serve as a guide in the study of the formation of the collective second-sound mode in the other two states of matter.

B. Solid bismuth

In this section we present some of our data on the propagation of heat pulses in bismuth. We show data from different crystallographic orientations and show how the collective mode forms from the individual single-particle-like ballistic modes.

As mentioned in the experimental section, the samples used in our heat-pulse work were known to have long electron mean free paths as they had been previously used in electron-wave experiments. Altogether, measurements were made on five different samples with resistance ratios $R_{300}/R_{4.2}$ of between 100–400. Most of the experiments reported here were done on two different samples labelled Bi I and Bi III where second-sound signals could be pursued to quite high temperatures before resistive processes took over. The measurements were made between 1.2 and 4.2 K, a choice dictated by previous thermal conductivity measurements. The thermal conductivity of our samples I and III is not known, but measurements of similar BTL-grown samples by McNelly⁵⁴ revealed that their conductivity was comparable to that reported in pure samples of previous work.^{55,56}

In Fig. 9 we show some typical heat-pulse measurements as a function of temperature in Bi III. The slight sloping background observed here and

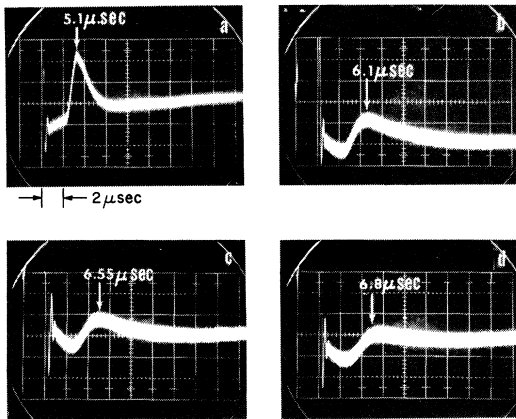


FIG. 9. Typical heat pulses in Bi III. Propagation length 5.1 mm. The pulses broaden and move to later time as temperature T is raised. Curve (a) 1.95 K; (b) 2.68 K; (c) 3.1 K; (d) 3.3 K. Propagation along C_3 axis.

in other directions (Fig. 12) is believed to be due to the semimetallic nature of the crystal. Possible electronic effects are presently being studied with laser-excited heat pulses. The propagation direction with the C_3 axis and the propagation length was 5.1 mm. At 1.4 K one observes only a single well-defined pulse whose propagation time of about 0.8 μ sec in excellent agreement with that expected for propagation of ballistic transverse phonons. The absence of longitudinal phonon in this direction is due to normal (N) phonon (hole) scattering.⁵⁷ Transverse phonons do not couple via N processes to the hole surface and Umklapp (U) processes are necessary. However, because of the small phase space available for U processes, the phonon mean free path is much longer than the propagation length. As the temperature is raised, the transverse pulse broadens and both the leading edge and peak retard in time. Above about 3.5 K the pulse begins to lose its form as diffusive (resistive) processes begin to dominate.

The qualitative behavior shown above is very similar to that observed in the transition region of formation of phonon second sound in liquid helium to be discussed later in Sec. IVC 1 and to the formation of sound in the gas discussed previously. The quantitative velocity-profile curve is also very similar to that described in the other two instances. The data are shown in Fig. 10 for bismuth III and bismuth I for two propagation lengths. It is clear from this figure that between 2.9 and 3.3 K the peak velocity approaches a *limiting value* of about 0.8×10^5 cm/sec. This is close to $(1/\sqrt{3})v_D$ (Debye velocity) calculated assuming $\Theta_D = 120$ K and expression (9) given earlier. The approach to this *limiting behavior* is a strong indication that the time retardation and broadening is due to N -process

scattering and not due to resistive processes. When these latter processes take over, the velocity reduces dramatically as is clear from the velocity profile data above 3.3 K. This will again be observed in the twofold axis data to be discussed later. From our data, it is also clear why Brown and Mathews⁵⁸ were unsuccessful in observing second sound in bismuth by the cw method. Their measurements were done at 4 K where resistive processes dominate even in the best of samples.

These points are further quantified through a calculation of the relaxation times τ_N and τ_R from our heat-pulse velocity-profile data. The calculated relaxation times as a function of temperature are shown in Fig. 11. These values of τ were calculated from the velocity data of Fig. 10 and expression (2) (in the absence of resistive scattering) and expressions (12) and (13) which take into account the finite resistive relaxation time. A best fit to the data were obtained with a normal-process relaxation time

$$\tau_N \approx 4.3 \times 10^{-5} T^{-4} \text{ sec.} \quad (20)$$

This value of τ_N differs from our earlier value⁸ because of an inadvertent omission of a factor of 2 previously. No explicit temperature dependence for τ_R is given because of the limited temperature range of the data where resistive scattering is significant. Nevertheless, it is clear from this figure that τ_R is a very steep function of temperature as is expected for U processes. Extrapolating the curves shown in Fig. 11, we estimate that these U processes will overtake the N processes at $T \sim 4.5$ K but, because of the exponential nature of the damping of heat pulses in the presence of resistive scattering, their effect can be felt for sam-

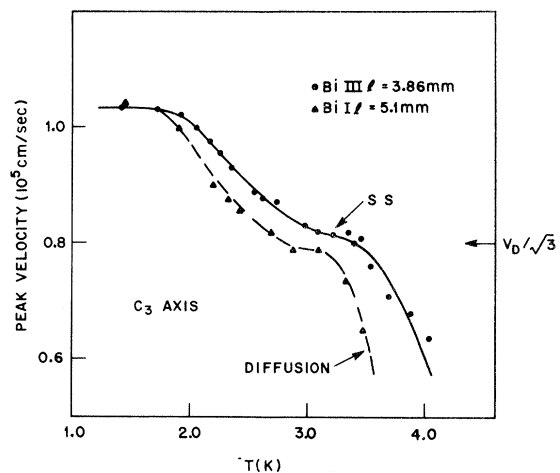


FIG. 10. Peak heat-pulse velocity as a function of T for two bismuth samples and two lengths. The limiting second-sound velocity is close to $(1/\sqrt{3}) \times$ Debye velocity (v_D) C_3 axis.

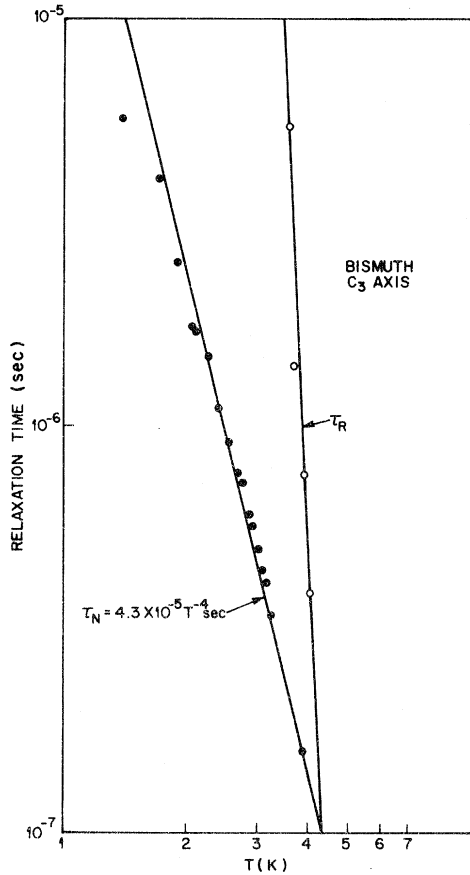


FIG. 11. Calculated normal-process relaxation time τ_N and resistive relaxation time τ_R . C_3 axis. Bi I.

ple lengths ~ 5 mm at $T \sim 3.5$ K, itself.

It is important to point out that the relaxation times given above are strictly valid only for T modes propagating in the C_3 direction. From analysis of thermal-conductivity data, Kuznetsov *et al.*⁵⁵ found that $\tau_N \sim 10^{-9}$ sec at 8 K. Our expression (20) yields a value $\sim 10^{-8}$ sec at 8 K. Though the numerical agreement is only fair, the temperature dependence of τ_N is the same in both cases. Our values of τ_R are, on the other hand, about a factor of 3 smaller than that estimated from thermal-conductivity data. These quantitative differences presumably arise from the highly directional nature of the heat-pulse experiments when compared with conductivity measurements. The phenomenological nature of the analysis of the data may also be the subject of some criticism.

We now turn to the orientation dependence of the heat-pulse data. In Fig. 12 we show our results for heat pulses propagating along the C_2 axis in Bi III. The propagation length was 5.6 mm. The shorter length enabled us to pursue the different modes as a function of temperature further than was possible in our earlier data.⁸ At low tempera-

tures we observed the ballistic propagation of all three modes. The relative amplitudes of these modes was in qualitative agreement with that estimated from phonon-focusing effects⁵⁹ and the density of states of the different modes. As the temperature was raised, all three ballistic modes decayed rapidly in intensity. In the vicinity of 3 K most of this intensity was transformed into a new mode, the second-sound mode, which arrived slightly later than the slow transverse (ST).

These features are illustrated somewhat more quantitatively in Fig. 13 where we have plotted both the signal intensity and the velocity behavior of the different modes as a function of temperature. The longitudinal (L) and fast transverse (FT) modes show little velocity variation but lose their intensity to the second sound (SS) mode which *apparently* grows out of the last ballistic mode (ST). Above 3.5 K this pulse again loses its form as diffusive processes set in. The saturated second-sound velocity is again about 8×10^4 cm/sec, close to $v_D/\sqrt{3}$. This again indicates that the final limiting second-sound mode is a thermodynamic mixture of all the modes of the system though the initial decay rates of the individual ballistic modes are different. This limiting behavior and the modal dependence of the intensities also reemphasize quite clearly that we are observing a well-defined second-sound mode free of impurity effects till about 3.5 K.

Finally, we wish to emphasize that all of the velocity profile data discussed so far are valid only in the limit of low-intensity heat pulses. If the amplitude is large, the heater temperature T_h is no longer a small perturbation from ambient and interaction effects set in even at $T_s \sim 1.4$ K. This is illustrated in Fig. 14 where we show the effect

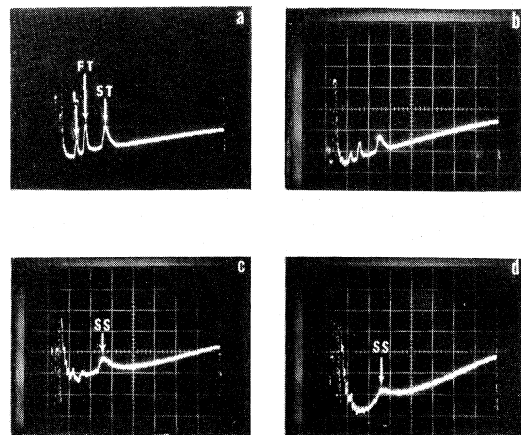


FIG. 12. Typical heat pulses in Bi III for propagation along C_2 axis as function of temperature. Curve (a) 1.62 K; (b) 2.12 K; (c) 2.85 K; (d) 3.52 K. Propagation length 5.6 mm. The decay of the ballistic modes into a single second-sound pulse is clearly seen.

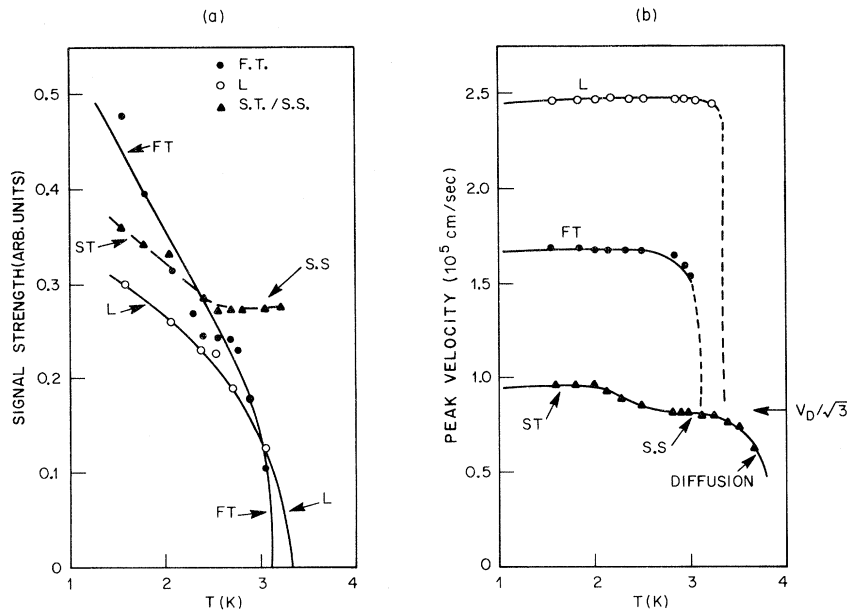


FIG. 13. Temperature dependence of (a) signal strengths and (b) peak velocities of heat pulses along C_2 axis. Bi III. Propagation length 5.6 mm.

of increasing amplitude. In addition to the usual ballistic pulse, we now see a slower component develop which increases in intensity as T_h is raised. At the highest heater powers, it dominates in intensity and now even an echo is clearly visible. We believe this additional pulse represents second-sound generated through the large temperature excursions of the heater. As the pulse propagates, it dilutes in intensity so that we observe a split pulse which consists of different fractions of ballistic and second-sound parts. We show these data to illustrate the effects of high amplitude. We shall see later that such behavior also occurs in liquid helium.

C. Liquid helium

In this section we summarize our experimental results on heat-pulse propagation in helium II as a function of temperature and pressure. Evidence for phonon second sound at SVP and roton second sound (at 24 bar) as well as the usual complete second sound at these pressures is presented. The implications of these experiments for the current theories of the lifetimes of the elementary excitations is discussed.

1. Phonon region

In Fig. 15 we show some typical low-temperature heat-pulse data at SVP over a propagation length l of ~ 0.23 cm. The data shown here were taken with a box car integrator and the typical pulse powers in this set were extremely low—about 3×10^{-3} W/mm² with a pulse width of about 8×10^{-7} sec. Data at high pulse energies showed substantial deviation from the behavior shown here and will be discussed

in a later section. At $T \approx 0.1$ K the leading edge arrival time of about $9.65 \mu\text{sec}$ of the main pulse corresponds to a velocity of about 238 m/sec, close to that expected for ballistic-phonon propagation. The peak velocity is also close to this value if one takes into account the finite pulse width. In addition to the main pulse, an echo at three times the

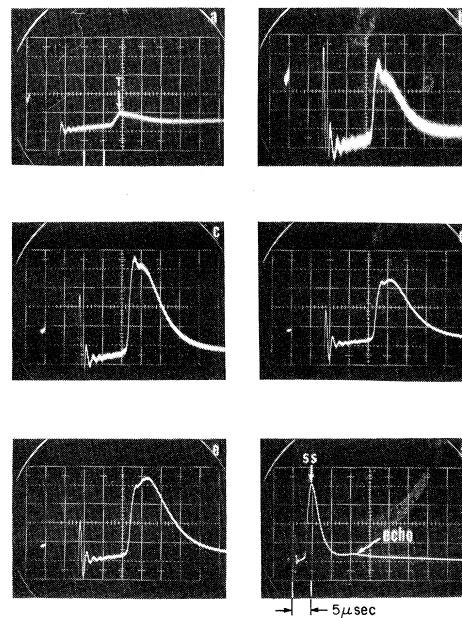


FIG. 14. Amplitude dependence of heat pulses in Bi III. Heater powers in W/mm²: (a) 0.024, (b) 0.25, (c) 1.5, (d) 2.85, (e) 3.95, (f) 6. Time scale (a)–(e) 1 μsec /(large division), (f) 5 μsec /(large division); ambient temperature ~ 1.4 K; input pulse duration 0.5 μsec ; heater area ~ 20 mm².

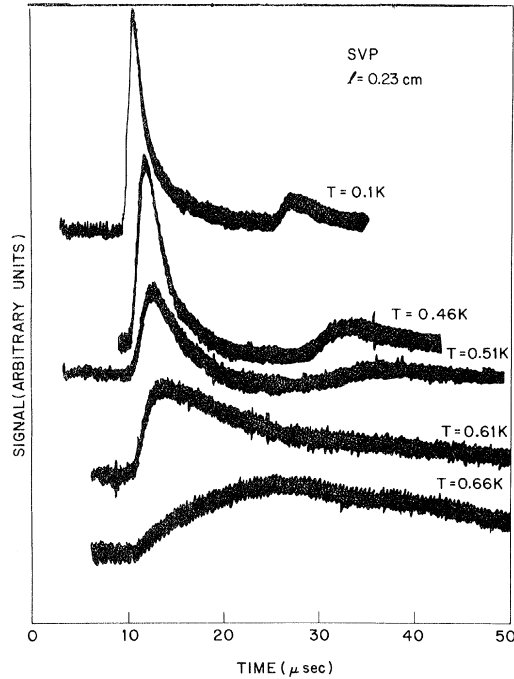


FIG. 15. Box car traces of temperature dependence of heat pulses in He II at SVP. Propagation length 0.23 cm. Phonon region. Note the time retardation and broadening of the heat pulse as the temperature is raised.

initial arrival time of this ballistic pulse is clearly detectable even at these low powers. No change is observed in the velocity of the detected heat pulses until $T \sim 0.35$ K. As the temperature is raised further, the ballistic pulse broadens rapidly and retards in a manner qualitatively similar to the C_3 -axis data for the solid bismuth. This broadening and time retardation are quite marked for the echo as well. Above about 0.62 K the pulse loses its form and at 0.66 K it is so broad that the peak velocity is ill defined. The peak velocity at 0.6 K is ~ 189 m/sec. Above about 0.75 K we see again well-defined pulses, this time with many echoes. These second-sound pulses have a velocity in agree-

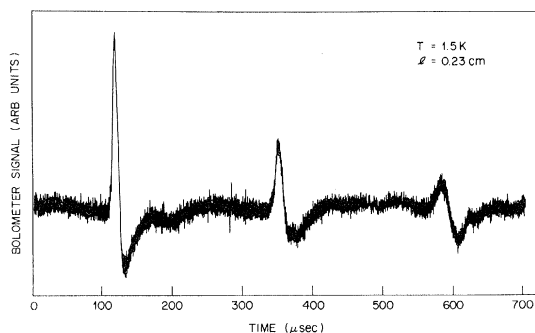


FIG. 16. Typical second-sound pulses in He II. $l = 0.23$ cm; $T = 1.5$ K.

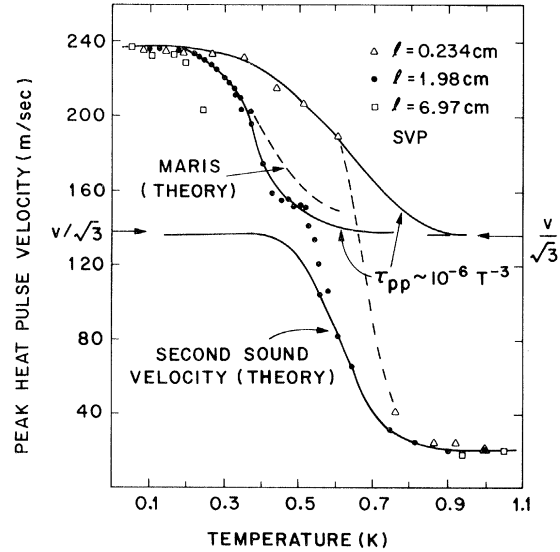


FIG. 17. Peak heat-pulse velocity in He II as a function of T at SVP for three different propagation lengths. At high temperatures excellent agreement with calculated second-sound velocities is obtained. The solid curves at low temperatures are best fits to the heat-pulse dispersion assuming Eq. (2) to be valid. The curve due to Maris is obtained from Ref. 49.

ment with previous data.¹¹ A typical second-sound pulse and its echoes are shown in Fig. 16. Again it is seen that the pulse shape reflects more the derivative of the initial pulse, in a very similar fashion to that observed for the sound wave in a gas.

In Fig. 17 we show the peak velocity as a function of temperature. The data for $l \approx 0.23$ cm are the triangles. The data for the larger cells will be discussed below. Also shown on Fig. 17 (solid line) is the calculation of the theoretical second-sound velocity from Eq. (5) assuming rapid interaction of all the excitations. It is clear that the velocity-profile curve for second sound in the entire gas of excitations agrees with the data only above about 0.75 K. The large change in velocity between 0.75 and 0.62 K is believed to arise because of the change in the phonon-roton scattering time τ_{pr} by at least an order of magnitude. From Fig. 5 we can see that τ_{pr} should change from about 3×10^{-7} to about 10^{-5} sec according to the calculation of Khalatnikov and Chernikova, i.e., the mean free path changes from a value of about $\frac{1}{30}$ of the sample length to greater than or equal to l for $l \approx 0.23$ cm. This again is consistent with our criteria that some 20–50 collisions are necessary for the formation of the collective mode.

Below about 0.55 K, $v_{ph} \tau_{pr}$ becomes more than an order of magnitude larger than 0.23 cm. The dispersion in the heat-pulse velocity must now arise from phonon-phonon scattering alone. It is clear

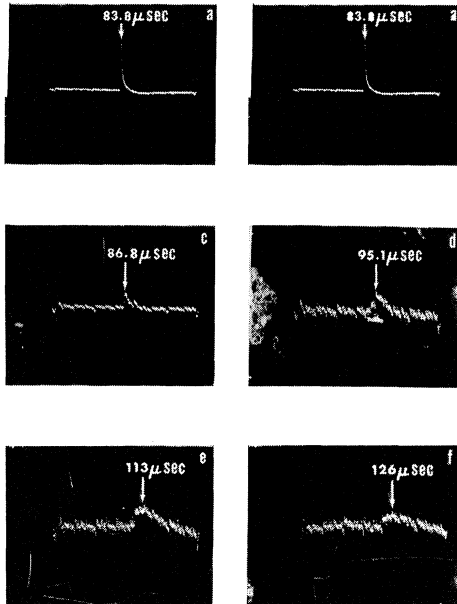


FIG. 18. Heat-pulse data in the 2-cm cell at low-power densities as a function of temperature. Curve (a) 0.1 K; (b) 0.24 K; (c) 0.27 K; (d) 0.35 K; (e) 0.40 K; (f) 0.45 K. Again note the broadening and time retardation as T is raised.

from Figs 17 and 1 that we reach a value of only $\omega\tau_{pp} \sim 1$ before the phonon-roton scattering process takes over. From Eq. (2) we find that the best fit to the data yields a value of $\tau_{pp} \sim 0.7 \times 10^{-6} T^{-3}$ sec.

From the above analysis it appears that considerably longer cells are required to reach the hydrodynamic (second-sound) regime in the phonon gas in helium II. In Fig. 18 we show data with a cell of length ~ 2 cm. These data were taken with the Biomation transient recorder and Fabritek signal averager. The power density to the heater was typically a factor of 5 larger than in the short cell. The extremely well-defined ballistic pulse arrives now at about 86 μ sec at $T = 0.1$ K. Quantitative intensity comparison with the short-cell data is difficult, but the signal appears about an order of magnitude stronger than for a $1/r^2$ radiator. This implies that the surfaces of our generators are sufficiently smooth so that part of the signal, in the ballistic regime, is concentrated in a narrow solid angle. Such behavior is similar to that observed with cleaved NaF by Sherlock *et al.*⁶⁰ and is due to the large difference in the sound velocity of the generator and the liquid. In the presence of a diffuse surface intensity varying as $1/r^2$ would be expected as has been observed by Guernsey and Luszczyński.¹⁴

As the temperature is raised above about 0.2 K, the heat pulse begins to broaden and retard in time rapidly. Some of these higher-temperature data

are also shown in Fig. 18. By 0.5 K the peak arrival time corresponds to a velocity of ~ 150 m/sec and appears to be reaching a limiting value similar to that observed in bismuth. This is more clearly illustrated through the velocity profile data of Fig. 17. The effect of the phonon-roton coupling occurs much earlier (around 0.53 K), and above ~ 0.6 K we get excellent agreement with the calculated second-sound velocity curves. The value of τ_{pr} is now estimated to be about 8×10^{-5} sec at 0.53 K. This is again in very good agreement with Fig. 5 and with our earlier data for $l \approx 0.23$ cm. The velocity-profile data for $l = 1.98$ cm in the phonon region yields a best-fit phonon-phonon scattering time $\tau_{pp} \sim 1 \times 10^{-6} T^{-3}$ sec. The temperature dependence is the same as that deduced from the short-cell data, but the numerical coefficient appears to be somewhat larger ($\sim 50\%$). Considering the limited region of the curve studied in the short cell, the agreement between the two sets of data must be considered good.

It is clear from the data shown in Fig. 17 that for $l \approx 1.98$ cm one is beginning to approach an onset to saturated-phonon second sound with $v_{II} \sim v_I/\sqrt{3}$ at $T \sim 0.5$ K. The approach to the limiting behavior encouraged us to do an experiment in a cell of length $l \sim 6.97$ cm. A typical ballistic pulse at $T \sim 0.07$ K is shown in Fig. 19. The heater power, here, was similar to that used in the 2-cm cell and from the signal strength it is again clear that the geometrical loss is small in the ballistic region. However, as the temperature is raised, the signal decays very quickly and above about 0.25 K no signal is detectable until very high temperatures (~ 0.8 K). This rapid decay in the phonon region is presumably due to the defocusing effect of three-dimensional phonon second sound in the transition region. The losses are now sufficiently great, and it appears from our data that the optimum length is ~ 2 cm, at least at SVP. This implies

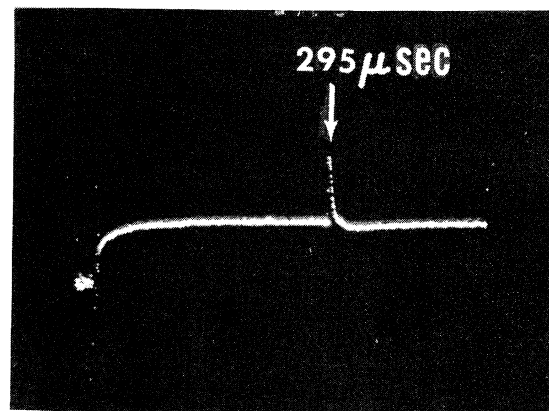


FIG. 19. Typical ballistic heat pulse observed in long cell. $l \approx 6.97$ cm; $T = 0.07$ K.

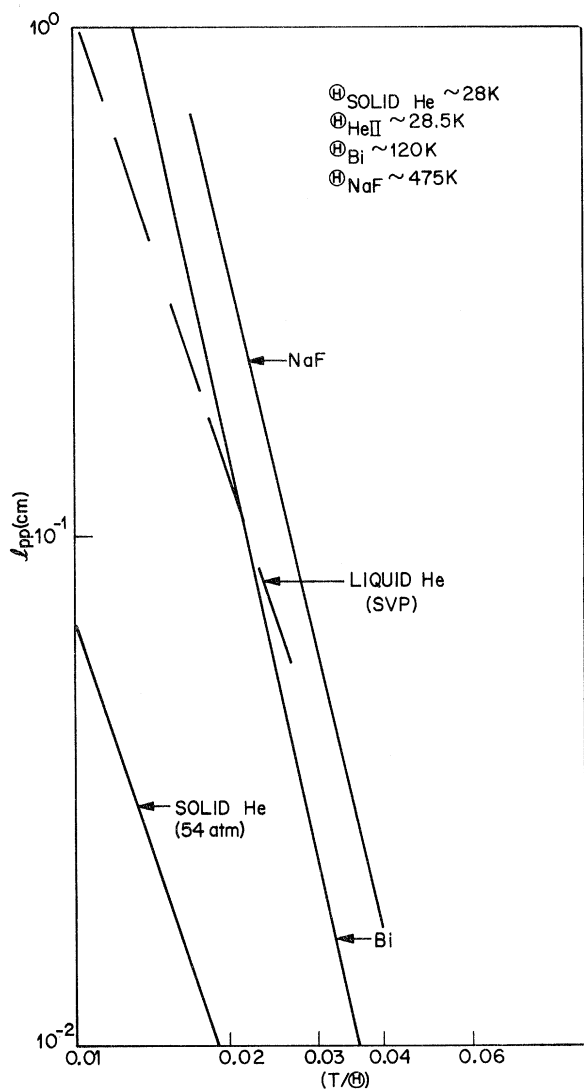


FIG. 20. Phonon-phonon mean free path l_{pp} plotted as a function of reduced temperature (T/Θ_D) . The data for solid He are those of Ackerman and Guyer (Ref. 63) and for NaF from Rogers (Ref. 17).

that an experiment such as that suggested by Saslow⁶¹ in chambers of $l \sim 10$ cm (so that one is in the true hydrodynamic regime) are not likely to be successful with presently available detector sensitivities.

The temperature dependence of τ_{pp} deduced in this work is slow compared with the T^{-5} dependence expected for the three-phonon process and T^{-9} dependence of the four-phonon process discussed in Sec. II B. Numerical values of τ_{pp} are in order-of-magnitude agreement with the τ_{pp}' estimated from Jäckle and Kehr's calculation, although the temperature dependence does not agree. In Fig. 17 we have also shown a theoretical plot due to Maris⁴⁹ (dashed line) for our 2-cm cell. We chose

the numbers from his refraction model since that is appropriate for our experimental situation, though the results of the isotropic model are not too different. His numerical values for the dispersion are higher than the experimentally observed values. In addition, his velocity profile appears to have an even slower temperature dependence than our experimental curves. This is presumably because the wide-angle process becomes effective only after numerous small-angle scatterings, and the velocity-profile curve is thus a complicated function of the parallel process rate and cannot simply be written in terms of a T^n dependence.

It is possible that the T^{-3} dependence is an artifact of our analysis since we are not always in the hydrodynamic regime. However, the numerical values obtained by us are close to that obtained by Whitworth from Poiseuille flow data (in the 0.4–0.6-K region). In addition, the T^{-3} dependence is remarkably similar to the T^{-3} dependence obtained by Ackerman and Guyer⁶³ for solid helium from both Poiseuille flow and second-sound data, where they were always in the hydrodynamic regime.

These points are brought out more clearly in Fig. 20 where we have plotted the mean free path $l_{pp} \approx v_p \tau_{pp}$ as a function of (T/Θ_D) . For⁶² SVP liquid He $C_v \approx 0.0207 \times T^3$ erg/gm °K which yields $\Theta_D \approx 28.5$ K. Thus most of our measurements are done for $T/\Theta_D \approx 0.022$ or below. For liquid He in the long cell the condition $l_{pp} < l$ is satisfied over a wide enough range in temperature, and the use of hydrodynamics is probably justifiable. Also shown in Fig. 20 are the values of τ_{pp} for solid helium⁶³ (at 54-atm $\Theta_D \sim 28$ K), Bi ($\Theta_D \approx 120$ K), and NaF ($\Theta_D \approx 475$ K). The similarity in the T dependences of the two common solids (NaF and Bi) and the two quantum systems (He) is to be noticed. It is also clear from Fig. 20 that for reasonable values of l , l_{pp} , and (T/Θ_D) only in solid helium is the scattering sufficiently strong to see sharp well-defined phonon second-sound signals with echoes. In liquid He and Bi, l_{pp} is at best $\sim \frac{1}{20}l$, so that one sees only the approach to a limiting behavior. Finally, in NaF l_{pp} is^{17,64} even longer and the limiting behavior is not achieved before other processes take over.

We now turn to the pressure dependence of the phonon-phonon scattering time in liquid He. The heat-pulse data for several different pressures are shown in Fig. 21 for $l = 1.98$ cm. The temperature data in the low-pressure region were more complete in the larger cell. It is clear that the variation in the heat-pulse velocity, in the phonon-dominated regime, with temperature, becomes less and less as the pressure is increased and becomes immeasurable at pressures above 10

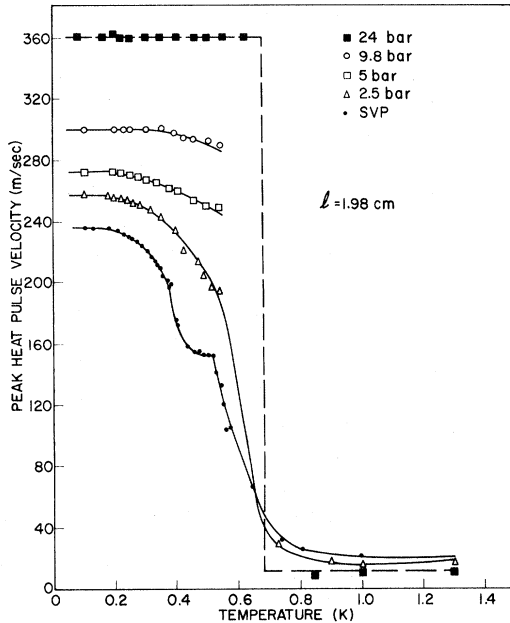


FIG. 21. Heat-pulse velocity as a function of temperature for five different pressures. Propagation length 1.98 cm. Liquid He II.

bar until $T \sim 0.70$ K. Below this temperature and for $p > 10$ bar the velocity of the leading edge of the ballistic pulses is in excellent agreement with the ultrasonic data. The velocities of the peak of the pulse and the leading edge are virtually the same (within about 2%) provided the amplitude of the pulse

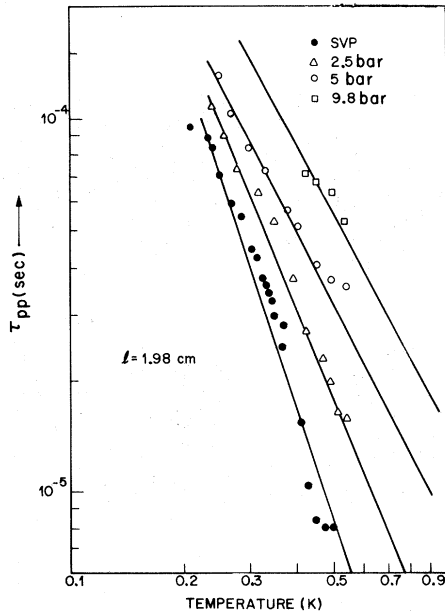


FIG. 22. Phonon-phonon scattering time τ_{pp} as a function of T for four different pressures. τ_{pp} was calculated from the data of Fig. 21 and Eq. (2). Liquid He II.

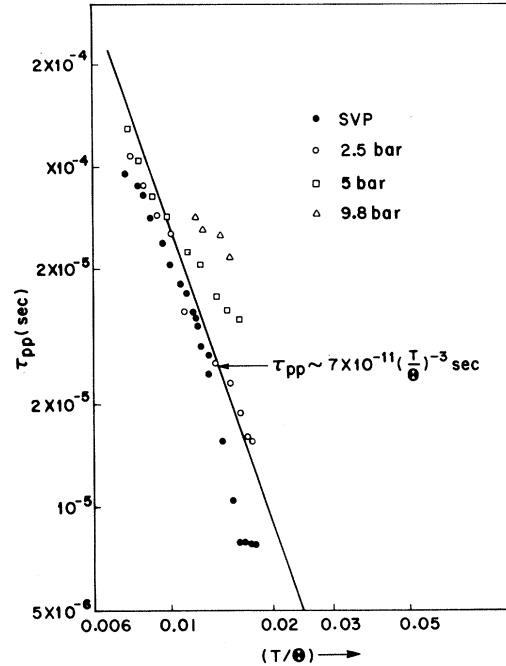


FIG. 23. τ_{pp} plotted as a function of reduced temperature (T/Θ) . Liquid He.

at the heater is kept sufficiently low. For large heater powers the peak velocity of the pulse is less than the ballistic leading edge due to the generation of higher-energy excitations which have a lower group velocity.

In Fig. 22 we have plotted the value of τ_{pp} as a function of T for pressures below 10 bar. These relaxation times were calculated from the velocity-profile data of Fig. 21 and Eq. (2). From Fig. 22 we can see that τ_{pp} increases by almost an order of magnitude (at fixed T) as the pressure is raised from SVP to 9.8 bar. The temperature dependence is still close to T^{-3} , though there seems to be some tendency for this power law to decrease even further as the pressure increases. It is difficult to be definitive on this point as the dispersion becomes weaker with increasing pressure. In Fig. 23 we have plotted τ_{pp} as a function of (T/Θ_D) with $\Theta_D = 28.5$ SVP and 36 K at 10 bar. A best fit to the data yields an approximate universal form for τ_{pp} ,

$$\tau_{pp} \sim (7 \pm 3) \times 10^{-11} (T/\Theta_D)^{-3} \text{ sec.} \quad (21)$$

The close similarity to the behavior of solid helium is to be noticed once more.

Above about 10 bar and below .72K the lack of variation in the heat-pulse velocity implies that $l_{pp} = v\tau_{pp}$ must be at least $\sim l$. This implies a value of $l_{pp} \sim 2$ cm or greater. The strong pressure dependence and the large increase in τ_{pp} as the pressure becomes large is qualitatively consistent with

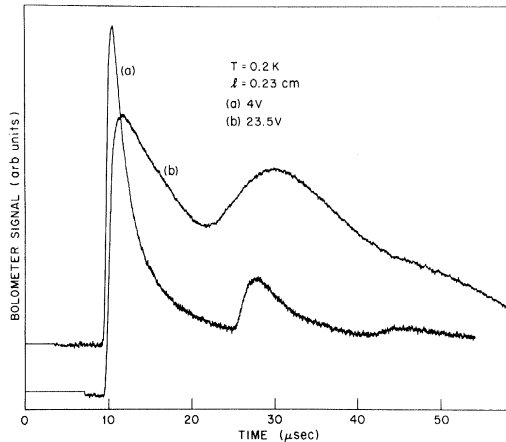


FIG. 24. Amplitude dependence of low-temperature heat pulses in liquid He at SVP. $T=0.2$ K; propagation length 0.23 cm. Curve (a) 4 V (0.023 W/mm²); (b) 23.5 V (0.79 W/mm²). Heater size ~ 14 mm². Pulse duration 0.2 μ sec.

the large increase in the dispersion parameter γ ($\gamma > 0$) in the phonon region of the He II excitation spectrum at high pressure, which effectively decreases the usual three-phonon scattering rate. In the low-pressure region the data are qualitatively consistent with the model of Jäckle and Kehr discussed earlier. Quantitative comparisons are not made at this time because our observed temperature dependence appears to be definitely different from that predicted by the different theories discussed earlier.

Finally, from the data shown in Fig. 21 it appears that the temperature of occurrence of the transition from phonon flow to complete second sound is almost independent of pressure. This temperature (0.62 – 0.75 K for $l=0.234$ and 0.55 – 0.68 K for $l\approx 2$ cm) regime though becomes narrower as the pressure is raised. Thus it appears that the phonon-roton scattering time τ_{pr} is at most very weakly pressure dependent. This is consistent with our earlier theoretical discussion and the model of Khalatnikov and Chernikova [Eq. (15)] where we saw that the effect of the increase in the roton number density with increasing pressure is almost exactly cancelled by the v^{-7} dependence of τ_{pr}^{-1} .

The consequences of the above values of τ_{pr} and τ_{pp} as a function of pressure for the observation of separate phonon and roton contributions to the heat flow is discussed in Sec. IV C3. We first turn to the effect of high heater powers on heat-pulse propagation at low ambient temperatures.

2. Amplitude effects in phonon region

The data discussed in Sec. IV. C1 are valid only in the limit of very low heater pulse powers

($\lesssim 1$ to 5 W/cm²) and pulse widths ($\lesssim 0.75 \times 10^{-6}$ sec). Thus it is clear that significant interactions set in at high enough pulse energies. The behavior to be discussed here is qualitatively consistent with that discussed before by Gueruzey and Luszczynski¹⁴ and Pfeifer and Luszczynski⁶⁵ but quantitatively different because of the much narrower pulse widths used in this work. The data are presented merely to show the type of effects to be expected at high energies with our generators and detectors, and they are to be carefully avoided to get meaningful data representative of thermal interactions.

In Fig. 24 we show the effect of very high amplitudes on the pulse shape in the short cell. It is clear that at the high amplitudes the ballistic pulse and its echo carriers only a small fraction of the total energy, a large part of which is contained in a broad diffusive type pulse. The leading edge of the ballistic pulse moves relatively little but the peak has moved significantly. This movement is probably a combined effect of dispersion (propagation of a significant number of high-frequency excitations with a group velocity less than the sound velocity) and the effect of interaction among the high density of generated excitations.

In Fig. 25 we show the effects of high amplitudes on the pulse shape in the $l \approx 2$ -cm cell. At high amplitudes a well-defined pulse with a peak velocity ~ 200 m/sec at SVP develops. The relative intensity of the second pulse increases markedly with amplitude though its velocity does not change significantly. With increasing ambient temperature, the two pulses merge and eventually form the second sound. The velocity-profile data shown in Fig. 26.

The velocity and behavior of this pulse is similar

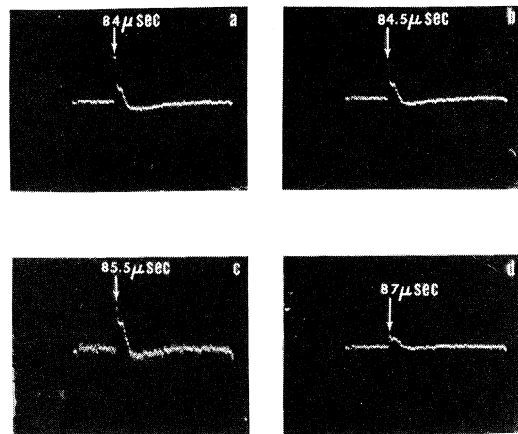


FIG. 25. Temperature dependence of heat pulse at high amplitude. Heater size ~ 14 mm²; pulse duration 1.2 μ sec. Heater voltage 12 V. Curve (a) $T=0.18$ K; (b) $T=0.22$ K; (c) 0.25 K; (d) 0.27 K. As the temperature is raised the ballistic pulse and the slower second pulse slowly merge into one. Propagation length ~ 2 cm.

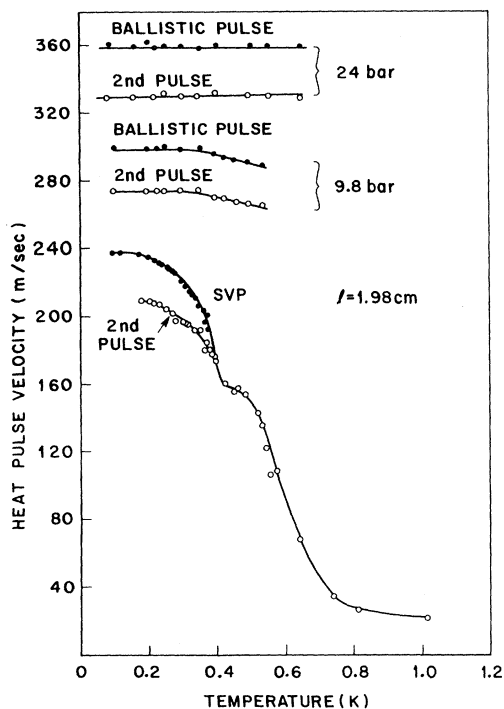


FIG. 26. Temperature dependence of velocity of second pulse (the ballistic pulse behavior is also included for comparison) at three different pressures.

to that reported by Guernsey and Luszczynski in their experiments. We believe it arises because of initial generation of second sound at these high amplitudes. In the large cell this pulse quickly dilutes itself and travels ballistically after probably a wall reflection. The lack of amplitude dependence of the velocity is consistent with generation of second sound above 0.7 K. The wall reflection and dilution is necessary since this behavior is observed only in the $l = 2$ -cm cell where wall reflections were not *entirely* avoided. The arrival time is consistent with a path incorporating a reflection off a wall unique to this 2-cm cell. These facts are also consistent with our high-pressure data. We find that, for example, at 24 bar we observe the ballistic pulse at 360 m/sec and the second pulse at ~ 325 m/sec as shown in Fig. 26. Since complete second sound occurs at about the same temperature at high and low pressures, the occurrence of the second pulse at all pressures at roughly a constant fraction of the ballistic pulse velocity is consistent with the above interpretation. If the second pulse had something to do with either the phonon or roton gases alone, we would have expected a dramatic pressure dependence which is not observed.

3. Roton region

In Sec. IV C1 we saw that the occurrence of complete second sound (involving the entire gas of

excitations i. e., phonons and rotons) occurs at approximately the same temperature at all pressures. From the theoretical curve for the second-sound velocity (Fig. 3) shown earlier it is clear that complete second sound should persist to lower temperatures at high pressures if τ_{pr} were sufficiently short. This is simply due to the fact that at 24 bar, the roton minimum $\Delta = 7.15$ K, while at SVP, $\Delta = 8.65$ K. However, from the data presented in C1 it is clear that the phonons at high pressure remain ballistic up to $T \sim 0.7$ K. This pressure independence of τ_{pr} implies that there is a "window" in temperature from about 0.45 to 0.7 K when the rotons are populated in significant numbers and yet are decoupled from the phonons at high pressures. In this section we present some of our measurements to observe this roton contribution to the heat flow.

Most of the measurements described here were done with the short cell. The bolometer in these experiments was a Sn/oxide/Sn tunnel junction placed in a magnetic field $H \approx H_c$. Even in these high fields the junction had a sensitivity somewhat better than the resistive indium bolometer used earlier.

Some typical heat-pulse data at 24 bar are shown in Fig. 27. The pulse amplitude and width were quite low and corresponded to energy dissipations ~ 10 erg/cm². At the lowest temperature, $T \sim 0.1$ K, only the single ballistic phonon pulse is observed. As the temperature is raised to about 0.4 K a new broad pulse arises at a time considerably delayed from the ballistic pulse. As the temperature of the sample is raised further this pulse sharpens and eventually between 0.7 and 0.8 K it merges with the usual second-sound pulse. The velocity profile curve for this new pulse is shown in Fig. 28. This velocity curve is identified

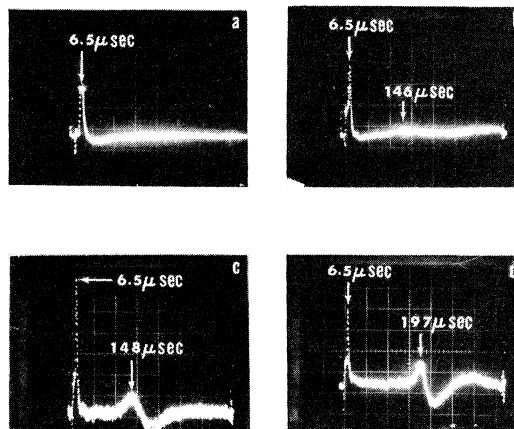


FIG. 27. Evolution of roton second-sound pulses in liquid He II at 24 bar. Curve (a) $T = 0.1$ K; (b) $T = 0.4$ K; (c) 0.55 K; (d) 0.65 K. Propagation length 2.34 mm.

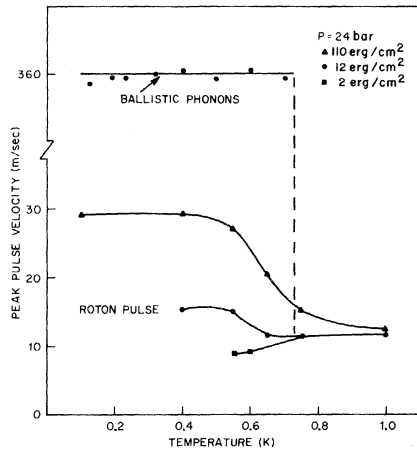


FIG. 28. Temperature dependence of "roton" pulse velocity for three different power levels into the heater. $P = 24$ bar; propagation length 0.234 cm.

with slow-moving roton components. In Fig. 28 we have also shown the velocity data for excitation energies as low as about 2 erg/cm² and as high as 110 erg/cm². The lowest-excitation-energy data were taken recently with an extremely sensitive junction and appears to be the limit of our sensitivity. At the higher excitation levels the "new" pulse appears at a lower temperature as nonthermal generation begins to occur.

The amplitude dependence of the velocity of the roton pulse is more clearly illustrated in Fig. 29. The ambient temperature for the data was about 0.55 K. Even though the error in the measurement is substantial [$\sim(20-30)\%$ of the velocity because of the large width of the pulse] it is clear that the limiting-zero-amplitude velocity is $\sim 7 \pm 2$ m/sec at 0.55 K. This value is extremely close to that expected for pure roton second sound as shown in Fig. 4. This interpretation is also consistent with both the "derivative" shape of the pulse and the expected short lifetimes for roton-roton interactions at this temperature. This lifetime is $\sim 10^{-6}$ sec according to Eq. (14) at these temperatures. Except for very high-velocity roton excitations, this lifetime yields a roton scattering length $\sim \frac{1}{100}$ of our sample length. At about 0.4 K this length increases by about an order of magnitude and the broadening observed at this temperature is probably the first indication of the finite roton lifetime. The highly dispersive nature of the velocity is also consistent qualitatively with the large amplitude dependence reported here. At the higher excitation levels one begins to generate a significant number of higher-velocity nonthermal roton excitations.

Liquid He II at various pressures and temperatures then affords the unique opportunity of studying both ballistic flow and second-sound flow in the gas of excitations. One can see phonon second sound

decoupled from the rotons; roton second sound decoupled from the phonons; and complete second sound in all excitations. This allows one to then estimate the various scattering times τ_{pp} , τ_{pr} , and τ_{rr} .

We have studied the nonthermal roton excitations in great detail as a function of pressure using a Sn "fluorescent" generator⁶⁶ and Sn tunnel detector. Their intensity, shape, and structure are found to depend greatly on the generated frequency. A detailed account of the complex structure observed in these experiments will be published in a subsequent paper.⁵⁰ In this paper we merely wish to show the gross features of roton second sound using heat pulses.

V. CONCLUSIONS

Using the fast-heat-pulse technique we have studied in detail the transition from second sound to ballistic phonon flow in liquid He II as a function of temperature, pressure, and propagation length. We have obtained numerical estimates of the wide-angle phonon-phonon scattering time τ_{pp}^{\perp} and shown that it depends strongly on pressure, in qualitative agreement with the theoretical model of Jäckle and Kehr. By the application of pressure we have also been able to vary the phonon and roton contributions to the heat flow. This has enabled us to observe the propagation of rotons decoupled from the phonons.

We have given a unifying discussion of second sound in terms of the elementary excitations. The onset of phonon second sound in liquid He II at SVP has been observed. The broadening and time retardation of the heat pulse in He II in the phonon region is shown to be experimentally similar to the onset of this mode in the solid bismuth and to the

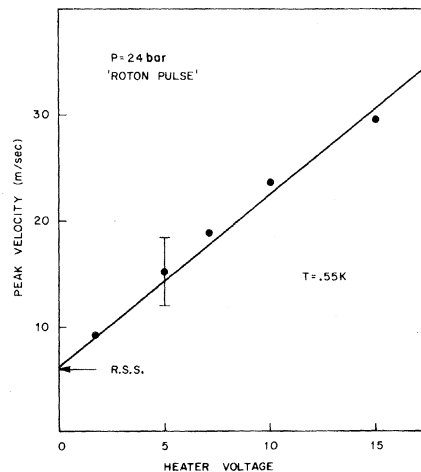


FIG. 29. Amplitude dependence of peak velocity of roton pulse. $T = 0.55$ K; $P = 24$ bar. The zero-amplitude velocity is close to that expected for pure-roton second sound.

transition from ballistic particle flow to sound in a gas (He⁴). These latter measurements show, that for submicrosecond heat pulses to propagate with a velocity approaching that of second sound ($\sim v/\sqrt{3}$) one requires a mean free path of the excitations to have a value of the order of $\frac{1}{2}l$ (within a factor of 2). Finally, even in a highly elastically anisotropic solid such as bismuth the velocity of second sound is within experimental error, independent of orientation, although the decay rates of the individual ballistic modes into the collective mode are quite different.

Considerable more work remains to be done.

The heat-pulse technique still suffers from the disadvantage that one is injecting a broad distribution (thermal distribution) and in a pulsed experiment one has many different Fourier components to deal with. Experiments using high-frequency sine waves and monochromatic sources (superconducting tunnel junctions) are presently under way. These should help in a quantitative understanding of the remaining open questions.

ACKNOWLEDGMENTS

The authors would like to thank M. A. Chin and J. P. Garno for their superb technical assistance.

- ¹L. Tisza, C. R. Acad. Sci. (Paris) 207, 1035, 1186 (1938).
- ²L. D. Landau, J. Phys. USSR 5, 71 (1941).
- ³L. D. Landau, J. Phys. USSR 11, 91 (1947).
- ⁴J. C. Ward and J. Wilks, Philos. Mag. 42, 314 (1951); 43, 48 (1952).
- ⁵E. W. Prohofsky and J. A. Krumhansl, Phys. Rev. 133, A1403 (1964).
- ⁶R. A. Guyer and J. A. Krumhansl, Phys. Rev. 148, 766 (1966); 148, 778 (1966).
- ⁷R. C. Dynes, V. Narayanamurti, and K. Andres, Phys. Rev. Lett. 30, 1129 (1973).
- ⁸V. Narayanamurti and R. C. Dynes, Phys. Rev. Lett. 28, 1461 (1972).
- ⁹K. Andres, R. C. Dynes, and V. Narayanamurti, Phys. Rev. A 8, 2501 (1973).
- ¹⁰For a recent review, see R. J. von Gutfeld, in *Physical Acoustics*, edited by W. P. Mason (Academic, New York, 1968), Vol. 5, p. 233. See also J. Phys. (Paris) 33, C-4 (1972).
- ¹¹V. P. Peshkov, Zh. Eksp. Teor. Fiz. 38, 799 (1960) [Sov. Phys.-JETP 11, 580 (1960)].
- ¹²K. R. Atkins and D. V. Osborne, Philos. Mag. 41, 1078 (1950); and H. C. Kramers, Proc. K. Ned. Akad. Wet. B 59, 35 (1956); B 59, 48 (1956).
- ¹³J. de Klerk, R. P. Hudson and J. R. Pellam, Phys. Rev. 93, 28 (1954).
- ¹⁴R. W. Guernsey and K. Luszczynski, Phys. Rev. A 3, 1052 (1971).
- ¹⁵V. Mayer and M. A. Herlin, Phys. Rev. 89, 523 (1953).
- ¹⁶R. J. von Gutfeld, A. H. Nethercott, Jr., and J. A. Armstrong, Phys. Rev. 142, 436 (1966).
- ¹⁷S. J. Rogers, Phys. Rev. B 3, 1440 (1971).
- ¹⁸C. S. Wang Chang and G. E. Uhlenbeck, in *Studies in Statistical Mechanics*, edited by J. de Boer and G. E. Uhlenbeck (North-Holland, Amsterdam 1970), Vol. 5, Pt. A.
- ¹⁹J. D. Foch, Jr. and G. W. Ford, in Ref. 18, Pt. B, p. 103ff.
- ²⁰The problem is also similar to the propagation of ion acoustic waves in gaseous plasmas. See, for example, I. Alexeff and R. V. Neidigh, Phys. Rev. 129, 516 (1963).
- ²¹M. Greenspan, J. Acoust. Soc. Am. 28, 649 (1956).
- ²²H. Palevsky, K. Otnes, and K. E. Larsson, Phys. Rev. 112, 11 (1958); D. G. Henshaw and A. D. B. Woods, *ibid.* 121, 1266 (1961).
- ²³P. J. Bendt, R. D. Cowan, and J. L. Yarnell, Phys. Rev. 113, 1386 (1959).
- ²⁴P. C. Kwok, Physics (L. I. City, N. Y.) 3, 221 (1967); and C. P. Enz, Ann. Phys. (N. Y.) 46, 114 (1968).
- ²⁵R. Cowley and A. D. B. Woods, Can. J. Phys. 49, 177 (1971); and A. D. B. Woods (private communication).
- ²⁶E. C. Svensson, P. Martel, and A. D. B. Woods, Phys. Rev. Lett. 29, 1148 (1972).
- ²⁷J. Brooks and R. J. Donnelly, Phys. Rev. A 9, 1444 (1973).
- ²⁸R. B. Dingle, Proc. Phys. Soc. Lond. A 65, 374 (1952).
- ²⁹J. A. Sussman and A. Thellung, Proc. R. Soc. Lond. 81, 1122 (1963).
- ³⁰See also the paper by Kwok (Ref. 24).
- ³¹J. Ranninger, Phys. Rev. B 5, 3315 (1972).
- ³²H. Beck and R. Beck, Phys. Rev. B 8, 1669 (1973).
- ³³L. D. Landau and I. M. Khalatnikov, Zh. Eksp. Teor. Fiz. 19, 637 (1949); 19, 709 (1949).
- ³⁴I. M. Khalatnikov, *Introduction to the Theory of Superfluidity* (Benjamin, New York, 1965).
- ³⁵J. Yan and M. J. Stephen, Phys. Rev. Lett. 27, 482 (1971).
- ³⁶J. Solana, V. Celli, J. Ruvalds, I. Tüttö, and A. Zawadowski, Phys. Rev. A 6, 1665 (1972).
- ³⁷H. B. Möller and L. Passell, Phys. Rev. (to be published); see also Ref. 25.
- ³⁸J. Jäckle and K. W. Kehr, Phys. Kondens. Mater. 16, 265 (1973).
- ³⁹I. M. Khalatnikov and D. M. Chernikova, Zh. Eksp. Teor. Fiz. 49, 1957 (1965) [Sov. Phys.—JETP 22, 1336 (1966)].
- ⁴⁰B. M. Abraham, Y. Eckstein, J. B. Ketterson, M. Kuchnir, and J. Vignos, Phys. Rev. 181, 347 (1969).
- ⁴¹C. J. Pethick and D. ter Haar, Physica (Utr.) 32, 1905 (1966).
- ⁴²J. Jäckle, Z. Phys. 231, 362 (1970).
- ⁴³H. Maris, Phys. Rev. A 8, 1280 (1973).
- ⁴⁴J. Jäckle and K. W. Kehr, Phys. Rev. A 9, 1757 (1974).
- ⁴⁵J. Jäckle and K. W. Kehr, Phys. Rev. Lett. 27, 654 (1971).
- ⁴⁶P. R. Roach, J. B. Ketterson, and M. Kuchnir, Phys. Rev. Lett. 25, 1002 (1970); and Phys. Rev. A 5, 2205 (1972).
- ⁴⁷P. F. Meier and H. Beck, Phys. Rev. A 8, 569 (1973).
- ⁴⁸S. G. Eckstein, as quoted in W. Saslow, Phys. Rev. A 5, 1491 (1972).

- ⁴⁹H. J. Maris, Phys. Rev. A 9, 1412 (1974).
- ⁵⁰R. C. Dynes and V. Narayanamurti, Phys. Rev. Lett. 33, 1195 (1974), and to be published.
- ⁵¹R. W. Guernsey, K. Luszczynski, and W. Mitchell, Cryogenics 7, 110 (1967).
- ⁵²I. Meyer and G. M. Sessler, Z. Phys. 149, 15 (1957).
- ⁵³G. M. Sessler, J. Acoust. Soc. Am. 38, 974 (1965).
- ⁵⁴T. F. McNelly (private communication).
- ⁵⁵M. E. Kuznetsov, V. S. Oskotskii, V. I. Pol'shin, and S. S. Shalyt, Zh. Eksp. Teor. Fiz. 57, 1112 (1969) [Sov. Phys.-JETP 30, 607 (1970)].
- ⁵⁶V. N. Kopylov and L. P. Mezhov-Deglin, Pis'ma Zh. Eksp. Teor. Fiz. Red. 14, 32 (1971) [JETP Lett. 14, 21 (1971)]. In very recent work these authors have obtained definite indications of Poiseuille flow with peak conductivities as high as about 40-W units {Zh. Eksp. Teor. Fiz. 65, 720 (1973) [Sov. Phys.-JETP 38, 357 (1974)]}.
- ⁷J. M. Ziman, Philos. Mag. 1, 191 (1956).
- ⁵⁸C. R. Brown and P. W. Matthews, Can. J. Phys. 48, 1200 (1970).
- ⁵⁹B. Taylor, H. J. Maris, and C. Elbaum, Phys. Rev. B 3, 1462 (1971).
- ⁶⁰R. A. Sherlock, A. F. G. Wyatt, N. G. Mills, and N. A. Lockerbie, Phys. Rev. Lett. 29, 1299 (1972).
- ⁶¹W. M. Saslow, Phys. Rev. A 5, 1491 (1972).
- ⁶²J. Wilks, *The Properties of Liquid and Solid Helium* (Clarendon, Oxford, 1967).
- ⁶³C. C. Ackerman and R. A. Guyer, Ann. Phys. (N. Y.) 50, 128 (1968).
- ⁶⁴T. F. McNelly, *et al.*, Phys. Rev. Lett. 25, 26 (1970); H. E. Jackson and C. T. Walker, Phys. Rev. B 3, 1428 (1971).
- ⁶⁵C. D. Pfeifer and K. Luszczynski, Phys. Rev. A 7, 1055 (1973).
- ⁶⁶R. C. Dynes and V. Narayanamurti, Phys. Rev. B 6, 143 (1972).

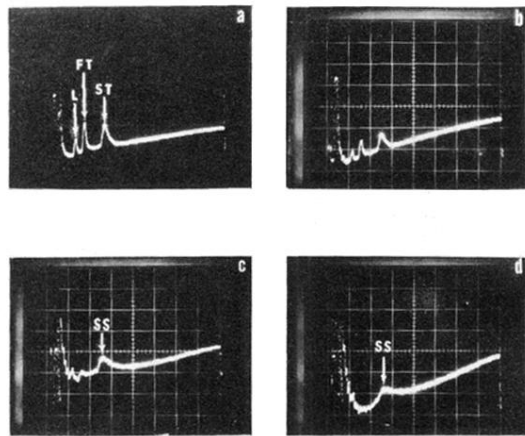


FIG. 12. Typical heat pulses in Bi III for propagation along C_2 axis as function of temperature. Curve (a) 1.62 K; (b) 2.12 K; (c) 2.85 K; (d) 3.52 K. Propagation length 5.6 mm. The decay of the ballistic modes into a single second-sound pulse is clearly seen.

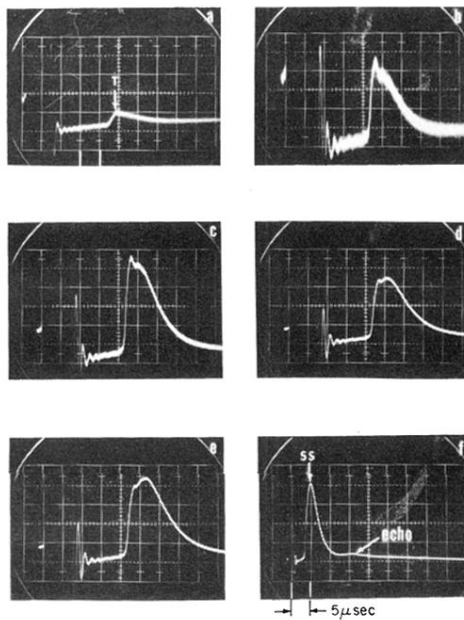


FIG. 14. Amplitude dependence of heat pulses in Bi III. Heater powers in W/mm^2 : (a) 0.024, (b) 0.25, (c) 1.5, (d) 2.85, (e) 3.95, (f) 6. Time scale (a)–(e) $1 \mu\text{sec}/(\text{large division})$, (f) $5 \mu\text{sec}/(\text{large division})$; ambient temperature $\sim 1.4 \text{ K}$; input pulse duration $0.5 \mu\text{sec}$; heater area $\sim 20 \text{ mm}^2$.

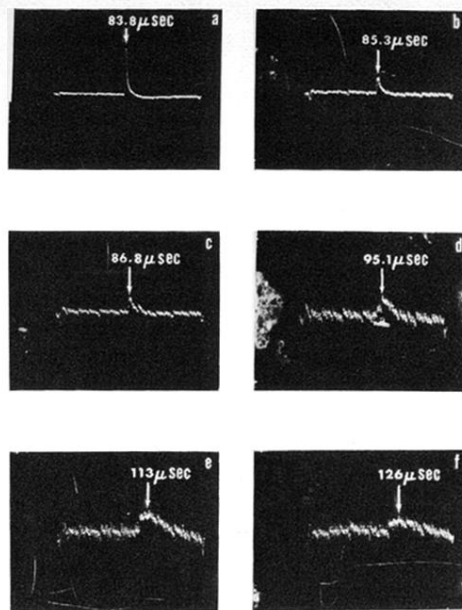


FIG. 18. Heat-pulse data in the 2-cm cell at low-power densities as a function of temperature. Curve (a) 0.1 K; (b) 0.24 K; (c) 0.27 K; (d) 0.35 K; (e) 0.40 K; (f) 0.45 K. Again note the broadening and time retardation as T is raised.

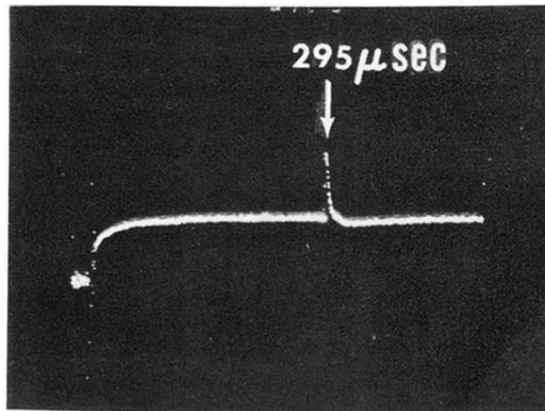


FIG. 19. Typical ballistic heat pulse observed in long cell. $l \approx 6.97$ cm; $T = 0.07$ K.

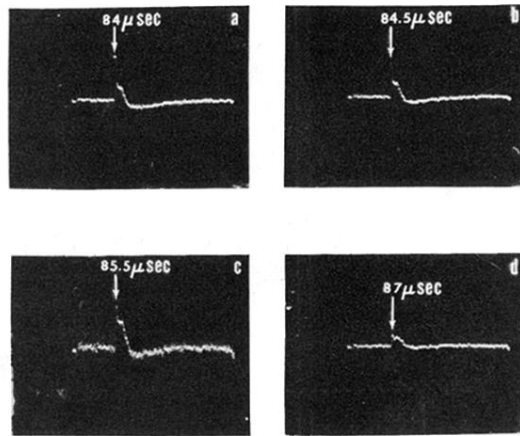


FIG. 25. Temperature dependence of heat pulse at high amplitude. Heater size $\sim 14 \text{ mm}^2$; pulse duration $1.2 \text{ } \mu\text{sec}$. Heater voltage 12 V. Curve (a) $T=0.18 \text{ K}$; (b) $T=0.22 \text{ K}$; (c) 0.25 K ; (d) 0.27 K . As the temperature is raised the ballistic pulse and the slower second pulse slowly merge into one. Propagation length $\sim 2 \text{ cm}$.

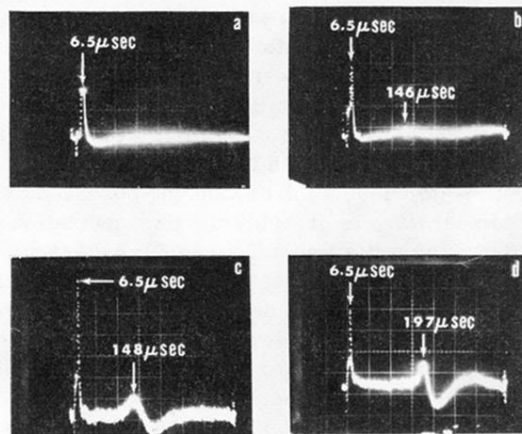


FIG. 27. Evolution of roton second-sound pulses in liquid He II at 24 bar. Curve (a) $T=0.1$ K; (b) $T=0.4$ K; (c) 0.55 K; (d) 0.65 K. Propagation length 2.34 mm.

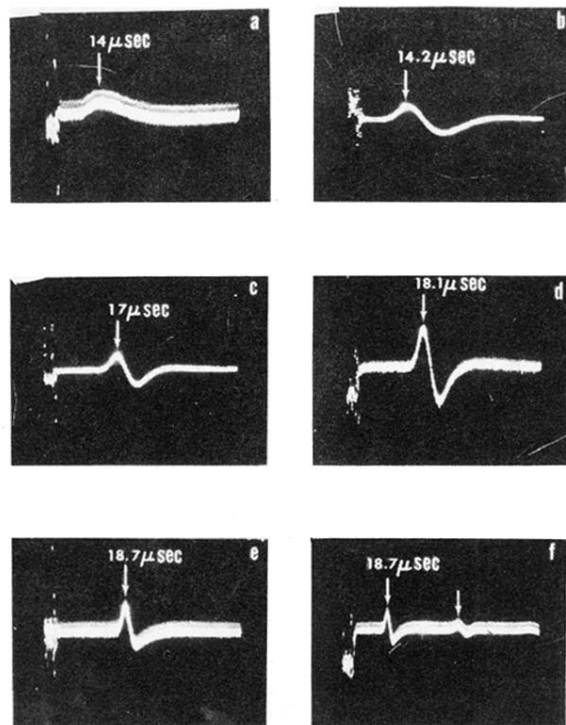


FIG. 7. Typical heat pulses in gaseous helium as a function of vapor pressure (in mtorr): (a) $<10^{-1}$; (b) 0.5; (c) 30; (d) 70; (e) 400; (f) 400. Propagation length, 2.25 mm; $T=4.2$ K.

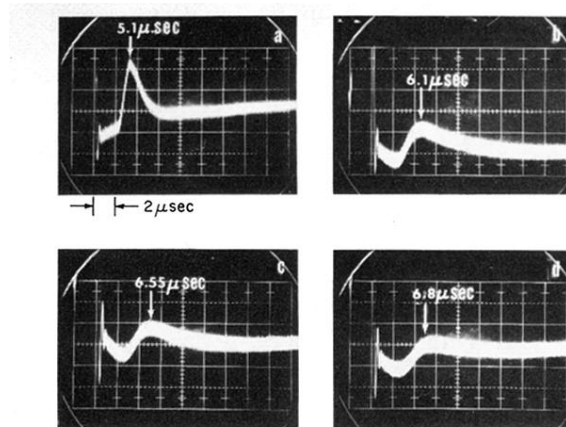


FIG. 9. Typical heat pulses in Bi III. Propagation length 5.1 mm. The pulses broaden and move to later time as temperature T is raised. Curve (a) 1.95 K; (b) 2.68 K; (c) 3.1 K; (d) 3.3 K. Propagation along C_3 axis.